DIRECT COOLING OF PROPULSION DRIVES FOR HIGH POWER DENSITY AND LOW VOLUME

Award No. N00014-01-1-0634

FINAL REPORT

REPORT DOCUMENTATION PAGE

Form Approved
OMB No. 0704-0188

1. REPORT DATE *(DD-MM-YYYY)*	2. REPORT TYPE	3. DATES COVERED *(From - To)*
30/03/2005	FINAL REPORT	01/04/2001 to 31/12/2004

4. TITLE AND SUBTITLE
Direct Cooling of Propulsion Drives for High Power Density and Low Volume - Award No. N00014-01-1-0634 N00014-01-0634: Final Report

5a. CONTRACT NUMBER

5b. GRANT NUMBER
N00014-01-1-0634

5c. PROGRAM ELEMENT NUMBER

6. AUTHOR(S)
J. C. Balda, F. D. Barlow, R. P. Selvam, A. Elshabini

5d. PROJECT NUMBER
01PRO7524-00

5e. TASK NUMBER

5f. WORK UNIT NUMBER

7. PERFORMING ORGANIZATION NAME(S) AND ADDRESS(ES)
University of Arkansas
Office of Contracts and Grants
120 Ozark Hall
Fayetteville, AR 72701

8. PERFORMING ORGANIZATION REPORT NUMBER

9. SPONSORING/MONITORING AGENCY NAME(S) AND ADDRESS(ES)
Mark S. Spector, Ph.D.
Office of Naval Research
Physical Sicences S&T Division, Code 331
800 N. Quincy Street, Arlington VA 22217-5660

10. SPONSOR/MONITOR'S ACRONYM(S)
ONR

11. SPONSOR/MONITOR'S REPORT NUMBER(S)

12. DISTRIBUTION/AVAILABILITY STATEMENT
Approved for public release, distribution unlimited

13. SUPPLEMENTARY NOTES

14. ABSTRACT
This final report summarizes the research work and conclusions related to ONR Award N00014-01-1-0634 under the DoD DESPCoR Program. The main objective of this grant was to investigate the feasibility of using spray cooling as the thermal management technolgoy for power semiconductor devices used in power converter applications. The report covers the following: Basics of spray cooling, a novel power packaging methodology for power semiconductor devices that it is compatible with spray cooling, the design of a power module serving as a technology demonstrator, and laboratory experimental results. Initial results seems to be superior to other approaches like cold-plate cooling.

15. SUBJECT TERMS
direct cooling, spray cooling, power packaging, power converters

16. SECURITY CLASSIFICATION OF:			17. LIMITATION OF ABSTRACT	18. NUMBER OF PAGES	19a. NAME OF RESPONSIBLE PERSON
a. REPORT	b. ABSTRACT	c. THIS PAGE			Juan Carlos Balda
UU	UU	UU	UU	40	19b. TELEPHONE NUMBER *(Include area code)* 479-575-6578

DIRECT COOLING OF PROPULSION DRIVES

FOR HIGH POWER DENSITY AND LOW VOLUME

Award No. N00014-01-1-0634

Period of Performance: April 01, 2001 – December 31, 2004

FINAL REPORT

Juan Carlos Balda, Fred D. Barlow, Panneer Selvam, Aicha Elshabini

University of Arkansas
Department of Electrical Engineering
3217 Bell Engineering Center
Fayetteville, AR 72701–1201
(479) 575-3005

Prepared for

Office of Naval Research
Ballston Center Tower One
800 North Quincy Street
Arlington, VA 222A-5660

March 2005

REPORT SUMMARY

DIRECT COOLING OF PROPULSION DRIVES FOR HIGH POWER DENSITY AND LOW VOLUME

Award No. N00014-01-1-0634

Background

Thermal management is presently a major issue in the power electronics field due to the exponential rise in power densities, and hence, increases in loss density and device temperatures. The ever escalating thermal management problems will not be resolved unless power semiconductor devices are able to operate at high temperatures (e.g., wide band-gap materials) or a packaging/cooling technology is developed that extracts effectively enormous amounts of waste heat from the electronics. Recently, spray cooling has gained much attention in various sectors because of its ability to manage anticipated future heat loads (> 100 W/cm^2).

Objectives

The main objective of this grant was to investigate the feasibility of using spray cooling as the thermal management technology for power semiconductor devices used in power converter applications, in particular, naval applications.

Approach

The approach followed by the researchers from the University of Arkansas (UAF) was the following:

- To understand the basics of spray cooling modeling involving phase change since previous research efforts have been mainly experimental with little research done on a comprehensive modeling of the phenomenon.
- To develop a power packaging methodology for power semiconductor devices that it is compatible with spray cooling. The research team felt that: *(a)* spray droplets impacting directly wire bonds and bare die might affect adversely the reliability, and *(b)* the thermal resistances between the bare die and the base plate must be reduced to maximize the benefits of spray cooling.
- To develop a power module as part of a technology demonstrator. The research team decided to develop an H-bridge topology to drive a dc motor.
- To perform thermal modeling of the H-bridge power module to aid in the design stages.
- To design and build a spray box for the developed power module that includes not only a module but also the gate drivers.
- To test the technology demonstrator in a laboratory environment.

Insulated Gate Bipolar Transistors (IGBTs) were selected as the power semiconductor device of choice because of their availability in bare die form from manufacturers at reasonable costs and the suitability of this semiconductor type for high power applications up to 2 MW power ratings.

Conclusions

The conclusions could be divided into two groups; namely, those related to spray cooling including theoretical and experimental ones, and those related to power packaging for spray-cooled power semiconductor devices.

Within the first group, the researchers established that

- The whole process of modeling phase change under spray cooling is a difficult task.

- Modeling of the heat transfer mechanism by a single droplet on a hot surface using a heat transfer coefficient and a CFD package has limited application because of the difficulty in determining the heat transfer coefficient under spray cooling from experimental work.
- Multiphase flow modeling is a viable technique to understand heat removal at the interfaces of liquid and solid by a vapor bubble.
- The "level set" method is one of the best methods to solve multiphase flow in spray-cooling systems.
- High nozzle flow rates are helpful when all other conditions are the same because of the enhanced conduction mechanism for heat removal. However, high-flow nozzles do not always produce the optimum cooling efficiency since they may hinder the phase-change process.
- Droplet size, droplet velocity and perhaps other factors clearly play a key role in this process. It is a challenge to relate theoretical variables such as droplet size and droplet velocity to variables that are used in the design of spray-cooling systems.
- Spray cooling is much better than liquid cooling of a standard TO-220AB package containing IGBTs.

Simply spraying a conventional power module does not result in the optimum cooling efficiency. The package must be also optimized. Within the second group of conclusions, the UAF researchers accomplished the following:

- Eliminated wired bonds, a major source of failure in power modules, by replacing them with solder balls.
- CTE matched the package materials for high reliability.
- Reduced the thermal resistance between the heat source and the liquid spray significantly, and thus improving overall cooling efficiency.
- Developed a power packaging technology suitable for chip-scale packages so power density can be increased further.
- The initial testing of the spray-cooled UAF power package far exceeded the performance of the liquid- or even spray-cooled conventional package.

TABLE OF CONTENTS

DIRECT COOLING OF PROPULSION DRIVES

FOR HIGH POWER DENSITY AND LOW VOLUME

I. INTRODUCTION

This Final Report summarizes the research work and conclusions related to Award N00014-01-1-0634 from the Office of Naval Research (ONR) under the DoD Experimental Program to Stimulate Competitive Research.

The research team from the University of Arkansas at Fayetteville (UAF) consisted of Drs. J. C. Balda, F. D. Barlow, R. P. Selvam (Computational Mechanics Laboratory), A. Elshabini, V. Wang and K. C. Burgers from the Department of Electrical Engineering and graduate students Mr. Kiran Vanam (doctoral candidate), Mr. Jeremy Junghans (MS candidate), Ms. Sandya Bhaskar (MS candidate), Mr. Suchit Reddy Damugatla (MS candidate) and Mrs. Y. Wei (MS candidate). The four co-principal investigators were Dr. Balda, Dr. Barlow, Dr. Selvam and Dr. Elshabini. Dr. Wang helped with packaging experimental issues and Dr. Burgers designed a gate driver for Insulated Gate Bipolar Transistors (IGBT). Ms. Bhaskar worked on theoretical understanding of the spray cooling phenomenon. Mr. Junghans developed the design of the spray-cooling system and Mr. Vanam the packaging methodology for spray-cooled power modules. Mr. Damugatla produced Flowtherm™ thermal models of a spray-cooled H bridge. Mrs. Wei selected the cold plate to compare the performance of a packaged IGBT when cooled by the cold plate versus the spray-cooling system.

Thermal management is presently a major issue in the power electronics field due to the exponential rise in power densities, and hence, increases in loss density and device temperatures (see Azar 2002). The ever escalating thermal management problems will not be resolved unless power semiconductor devices are able to operate at high temperatures (e.g., wide band-gap materials) or a packaging/cooling technology that extracts effectively enormous amounts of waste heat from the electronics. Recently, spray cooling has gained much attention in various sectors because of its ability to manage anticipated future heat loads (> 100 W/cm^2). Thus, the main objective of this grant was to investigate the feasibility of using spray cooling as the thermal management technology for power semiconductor devices used in power converter applications, in particular, naval applications. From the initial research activities, the research team established the following enabling objectives:

- Understand the basics of spray cooling modeling involving phase change since previous research efforts have been mainly experimental with little research done on a comprehensive modeling of the phenomenon.
- Develop a power packaging methodology for power semiconductor devices that it is compatible with spray cooling (i.e., it was thought that spray droplets impacting directly wire bonds and bare die might affect adversely the reliability). Previous research efforts have sprayed the base plate of the power module; thus, the thermal resistance of the package remained unaltered (see Shaw (2002)). The research team felt that the thermal resistances between the bare die and the base plate must be reduced to maximize the benefits of spray cooling. IGBTs were selected as the power semiconductor device of choice because of their availability in bare die form from manufacturers at reasonable costs and the suitability of this semiconductor type for high power applications up to 2 MW power ratings.
- Develop a power module as part of a technology demonstrator. The research team decided to develop an H-bridge topology to drive a dc motor. The latter was chosen because of its simplified control requirements (as opposed to those for an induction motor). The goal was to

evaluate the feasibility of spray cooling as a thermal management tool for power semiconductor devices independently of the driven electric motor.

- Perform thermal modeling of the developed H-bridge power module to aid in the design stages.
- Design and build a spray box for the developed power module that includes not only a module but also the gate drivers (which were designed using off-the-shelf components).
- Test the technology demonstrator in a laboratory environment.

This final report is organized as follows: Section I provides a general overview of the research team and the project objectives, Section II presents the status of computer modeling of the spray cooling phenomenon during the period of performance of the award, Section III describes the philosophy developed for packaging power semiconductor devices subjected to spray cooling, Section IV briefly summarizes thermal modeling of the H-bridge module using Flowtherm™, a Computational Fluid Dynamic (CFD) software package which allows simplified simulation of the spray cooling phenomenon, Section V describes the design and construction of a spray cooling box for a H-bridge power module intended to drive a dc motor, Section VI presents the experimental results, Section VII provides the conclusions of the research work enabled by this ONR research grant, and finally, Section VIII provides a brief summary of future work by the UAF researchers.

II. COMPUTER MODELING OF SPRAY COOLING

For efficient design of spray cooling systems, understanding of the spray dynamics and droplet evaporative cooling phenomenon via numerical simulation is very important. The entire physical processes associated with this phenomenon are very complex. The processes ranging from the time the fluid comes out of a nozzle orifice as spray of fine droplets that will impinge on a hot surface and vaporize to the time that the vapor is removed have to be modeled accurately. There is not much theoretical work done to theoretically understand the spray cooling in the two-phase regime on a closed-loop system using a pure single component medium such as water or Fluorinert™ fluids without the use of air as atomizer fluid. Some related discussion is found with regard to fuel-air spray in automobile engine combustion as reported by Srignano (1999). DiMarzo (1993) modeled the evaporation of a droplet from a hot surface for different applications. Several other modeling efforts are reported in the literature with regard to the effect of the impact on the droplet, associated shape change mechanism, and other issues. The status of spray cooling was surveyed as part of this ONR award with a summary given below. Conclusions and future work on theoretical understanding and computer modeling of spray cooling to be addressed in a followed up Phase II project (ONR Award No. N00014-04-1-0603) are given in Sections VII and VIII.

II.1 Effect of a Single Droplet on Heat Transfer Using Heat Transfer Coefficient

The effect of a single droplet on heat transfer was first modeled as the beginning to theoretically understand the spray cooling phenomenon. The interface between the droplet and vapor was modeled using a moving boundary similar to the work reported in Gordon (1999) and DiMarzo (1993). So the amount of liquid vaporized at the interface of the liquid-vapor is taken away from the droplet at each computing time. DiMarzo measured experimentally the convective heat coefficient to be used for modeling purposes. Their modeling assumed that the vaporization happened at the interface of the liquid-vapor. Whereas in the real world, depending on the size of the droplet, evaporation can happen through several mechanisms and a vapor bubble can form at the interface with the liquid or at an interface involving solid and liquid. Other models were investigated since the reported liquid-vapor model is not representative of what is actual happening in the spray-cooling phenomenon.

II.2 Theoretical Issues in Spray Cooling

There are several theoretical challenges at this time ranging from the efficient design of jets to convert the liquid into spray and finally the process of removing the heat from the hot surface. There is no comprehensive theoretical model available at this time for spray cooling that includes phase change. Hence, there are no CFD packages which the researchers or end users can commercial obtain for this application. Complete modeling of the heat removal by micro jet array system using the Finite Difference Method (FDM) for a single fluid was reported by Selvam and Elshabhini (2000). Availability of similar models for spray cooling should be a valuable tool for the design of spray-cooling systems. Tryggvason et al. (2001) gave a general review of multiphase flow modeling including current limitations as well as specific developments in the front-tracking method used for multiphase flow simulation. They discussed the application of the model to bubbly flows, atomization of liquid for combustion, secondary breakup of drops, primary breakup of a jet, solidification and boiling flows. This is a good survey paper for a beginner in this area. Dhir (2001) gave a summary of their numerical simulation for pool boiling heat transfer including some issues related to microgravity environments. Particular technical issues are specifically addressed in the next few sections.

II.2.1 - Flow in spray nozzle: Rahman (2004) analyzed the single-phase flow in a swirling jet using a Finite Element Method (FEM) for optimum design. The numerical simulation predicts the jet cone angle and pressure drop across the nozzle. Further work is needed to consider the formation of the spray and its effect in the design of jets.

II.2.2 - Atomization of droplet: Tryggvason (2001) gave a survey on computer modeling of atomization of droplets. The methods were classified into two groups: primary breakup and secondary breakup. Few researches including Tryggvason's group work were reported. A general survey on drop and spray formation from a liquid jet was provided by Lin and Reitz (1998) including the status of experimentation and modeling.

II.2.3 - Droplet and surface interaction: Kizito (2004) used the Tryggvason's front tracking model to study the splashing droplet on a hot plate. They found that the maximum heat is transferred on the substrate when the droplet has the widest extent of spread. Pasandideh-Fard (2001) used the Volume of Fraction (VOF) method for similar work. In these two references the fluid is below the range of boiling and they both used a droplet having a 2-mm diameter.

II.2.4 - Liquid and vapor interaction or bubble dynamics: Extensive computer modeling work has been done in this area. The surveys of Tryggvason (2001) and Sussman (1994) are significant contributions. Here, surface tension and gravity have an impact on the dynamics of the bubble in the liquid. The shape of the bubble can change depending upon which factor dominates. There is extensive knowledge available in this area. This is part of the boiling flows and spray cooling when vapor grows as a bubble and moves in the liquid.

II.2.5 - Liquid, vapor and surface interaction on a hot surface or boiling flows: The phenomenon of nucleation during boiling and the growth of a vapor bubble on a hot surface are not well understood and only few modeling efforts have been initiated in recent years. The modeling efforts can be classified into two categories: *(1)* Multiphase flow modeling considering conduction, convection and phase change phenomena, and *(2)* Simplified procedures where only conduction and phase changes are considered. Welch and Wilson (2000), Son and Dhir (1998) and Juric and Tryggvason (1998) have computed the film boiling stage using multiphase flow modeling. This stage was modeled earlier even though it occurs after nucleate boiling. The reason might be that the density ratio is far smaller than that one in nucleate boiling situations. Some research work has been done on nucleate boiling and will be reported below.

II.2.5.1 - *Film Boiling*: Welch and Wilson (2000) used the VOF method to model film boiling. Juric and Tryggvason (1998) used the front-tracking method to study film boiling in 2D grids while Shin and Juric (2002) used it for 3D grids. They could only consider cases with low density ratios. The numerical method could not allow them to apply their approach for high density ratios that occur in nucleate boiling flows. Son and Dhir (1998) used the level set method, which is similar to the method in Sussman (1994), to compute film boiling. The computed results were in reasonable agreement with the experimental results.

II.2.5.2 - *Nucleate Boiling*: Lee and Nydhal (1989) computed the single bubble growth in nucleation boiling by considering only the liquid region and assuming the bubble to be spherical. Then, Son (1999) applied their film boiling model to compute bubble growth during nucleation boiling. The computed bubble size was around 1 mm and compared well with their experimental results. The bubble growth during nucleation in their model was mainly due to the micro region model which was based on a 1D model close to the dry out area on the hot wall. For the macro region where the Navier-Stokes equations were used, the contribution to phase change was very small. Bai and Fujita (1999) and Yoon (2001) also computed the nucleated pool boiling using the Lagrangian method for tracking the interface and considering only the liquid region. This approach was similar to that of Lee and Nydhal except the meniscus model in Bai and Fujita was close to Son (1999). Kunugi (2001) used the VOF method for boiling and condensation problem without much detail on the numerical implementation or the problems that were considered.

II.2.5.3 - *Simplified Models*: Di Marzo (1993) modeled a single water droplet on a hot surface. He (2001) proposed a model for boiling heat transfer based on a numerical macro-layer model. Here, the boiling curve was reproduced numerically by determining the macro-layer thickness. They explained that the evaporation due to the growth of vapor stem was the main contribution to the total heat flux. They combined this model with a conduction model for transient analysis. Stephan and Hammer (1994) and Kern and Stephan (2003) used micro and macro regions for modeling heat transfer during nucleation boiling. In the micro region, a 1D complex fourth-order equation was solved to determine the thickness and width of the region with only conduction considered in the macro region. They compared computed and experimental results.

II.2.6 - Spray cooling: From the above discussions one can conclude that several different research efforts have been undertaken to understand different phases of boiling and most of them were for pool boiling. None of them can be applied directly to the understanding of spray cooling. In the case of spray cooling which is of interest to electronic cooling, conduction of heat from the hot wall into the liquid, nucleation and growth of a vapor bubble on the hot surface due to phase change, convection of liquid and vapor bubble in the liquid film, and impact of a spray droplet on both the thin liquid film and a vapor bubble, all happen simultaneously as shown in Figure 1. The above processes happen in the midst of surface tension and micro or macro gravity conditions. Son (1999) could grow bubble diameters larger than 1.25 mm and moved them smoothly into a 7.5-mm pool of liquid above. Also, most of the phase change happened in the micro region.

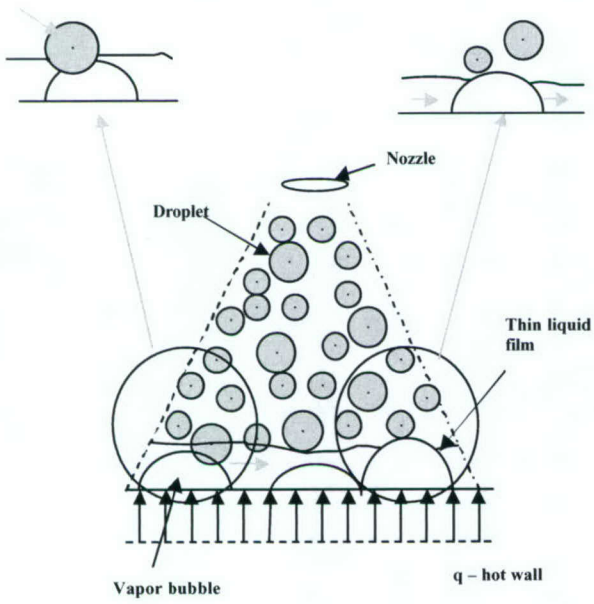

Fig. 1 Spray cooling phenomenon.

In spray cooling, it is very rare to have a liquid film thickness greater than a couple of millimeters. Furthermore, the liquid film on the hot surface will be in the range of 40 μm to 200 μm for spray-cooling systems designed for high heat fluxes. Usually the thickness can be about 20% of the diameter of the spray as observed by Kizito (2004) in their experimental and computer modeling work. Lin and Ponnappan (2003) reported around 40 μm and Rini (2002) reported in the range of 200 μm.

Theoretical understanding of the nucleate boiling in thin films in the range of 40 μm to 200 μm is not available at this time. As a start to understand the spray cooling phenomenon in a thin liquid film, the range of 70 μm will be considered by the UAF researchers. The growth of vapor bubbles and their impact on heat removal on the hot surface will be investigated in Phase II of this project on spray-cooling systems for power semiconductor devices.

II.3 Methods to Solve Multiphase Flow

The major classifications of methods to solve multiphase flow are the Lagrangian method, Arbitrary-Lagrangian-Eulerian (ALE) method and Eulerian method. Some of the applications of multiphase flow modeling using these methods will be discussed below with the advantages and disadvantages of each method. Tryggvason (2001) gave a comprehensive survey and Scardovelli and Zaleski (1999) presented a survey on VOF with discussions on numerical techniques. In the same journal volume of Tryggvason (2001), several other review papers on multiphase flow modeling are available and are very informative. The equations were solved using either FDM or FEM. Of these two methods, the FDM is the most popular one. The primary numerical procedure used by the UAF researchers is either FDM or FEM on equal grid spacing.

II.3.1 - Lagrangian method: This method is fairly complex as reported by Tryggvason (2001). The method was used for vapor bubble growth modeling by Welch (1998) using FEM and Lee and Nydhal (1989) for nucleate boiling using FDM on a body-fitted grid system.

II.3.2 - Arbitrary-Lagrangian-Eulerian method: Yoon (2001) applied the ALE procedure to study the bubble growth and departure from the heated surface. They used the mesh free method which is a recent development in engineering for the Eulerian calculations. The implementation may be complex when compared to FDM or FEM.

II.3.3 - Eulerian methods: Front capturing methods, the separate boundary-fitted grid method for each phase, the front tracking method and the hybrid of front-tracking and front-capturing methods are available at this time for multiphase flow calculations as reported by Tryggvason (2001). The primary methods used in front capturing approaches are the Marker and Cell (MAC) method, the VOF method, the level set method and the combination of VOF and level set methods. The separate boundary-fitted grid method is only suitable for simple geometries.

Of the methods mentioned above, the VOF method and level set methods are applied extensively in the literature for multiphase flow modeling. Discussions on VOF and level set methods are available from Ferziger and Peric (2002) and a good discussion on different applications of the level set method is given by Osher and Fedkiw (2003). In the VOF method, sharp differentials have to be calculated between the interfaces. The color function in the VOF method is solved using a time dependent convection equation. This is similar to computing shock flow in compressible flow analysis.

To alleviate the problem of calculating sharp differentials in the level set method, a distance function is introduced which will be varying gradually in each phase. The equation to be solved is the same as in the VOF method except the use of a distance function instead of the color function. Once the distance function is solved the color function is recovered from the sign of the distance function. The level set method is good for calculating interfacial curvature accurately but mass conservation is not satisfied. Combining with the VOF method this error is eliminated as reported by Son and Hur (2002). Also, it is easy to handle breaking and merging of an interface such as the liquid-vapor interface in the level set method. In addition, the implementation of 3D problems is a straight forward extension. Therefore, the level set technique was selected for interface capturing in the work forming part of a continuation project (that is, ONR Award No. N00014-04-1-0603).

III. POWER PACKAGING COMPATIBLE WITH SPRAY COOLING

Reliability may be compromised when spraying a liquid onto fragile wire bonds, which are a major source of failure for packages for semiconductor devices (see Ng 2000). If the spray can be kept perfectly clean this may be possible, however, in a real system the presence of impurities in even very small quantities will erode the surface of the die and wire bonds. As a result, the die must be protected. In addition, conventional packages were not developed to realize the full potentials of spray cooling. These packages contain considerable thermal resistance when compared to the low thermal resistance to the ambient provided by spray cooling.

In order to address these issues, the UAF researchers developed a novel packaging methodology to replace the conventional wire bonds and allow for the package to be directly spray cooled (Vanam 2005). The new packaging methodology enables an important reduction of the thermal resistance between the heat source and the sprayed fluid, thereby greatly improving the overall cooling efficiency. The UAF packaging team decided first to build a test vehicle employing a thermal test die to demonstrate both the potential of spray cooling for power electronics and the feasibility of the proposed packaging technology. The test vehicle, which consists of a thermal test die with built in temperature sensors, enabled the researchers to easily change the heat load and understand the spray cooling phenomenon under different scenarios. Finally, the packaging methodology was implemented in an H bridge, a benchmark circuit, using IGBTs from International Rectifiers (IR). The thermal capabilities of this H-bridge power module were demonstrated by driving a 240-V, 10-hp dc motor. A patent filing is under preparation for this power packaging methodology that is described next.

III. 1 ProposedPower Packaging Methodology

The proposed base package shown in Figure 2 consists of a heat spreader with the power semiconductor device (i.e., the IGBT) flip chipped onto a substrate such as DBC (Direct Bond Copper). The heat spreader not only provides an electrical path but also a good thermal path. A potting compound can be used for encapsulation of the power device. The top and bottom connections of the power device (IGBT) with the heat spreader and the DBC are created using a high temperature solder and a low temperature solder, respectively. The advantages of such an approach are:

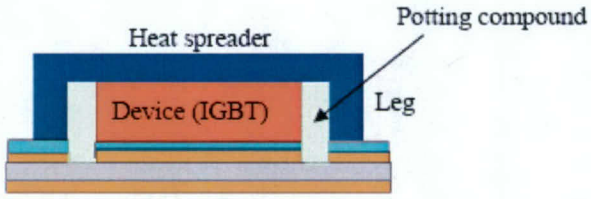

Figure 2. Proposed package compatible with spray cooling.

- Wire bond connections are eliminated
- Thermal paths are improved
- High heat fluxes in excess of 100 W/cm^2 are possible
- Double-side cooling is possible

Different variations of the base package are possible depending upon the choice of the heat spreader material. Some choices for the heat spreader material are diamond, Metal Matrix Composites (MMC), AlN, and CuMo. In the case of diamond or AlN, which are electrical insulators, modifications are required to achieve the top electrical connection (typically the collector connection for an IGBT). The package employing diamond/AlN as the heat spreader is shown in Figure 3. In this package, the kovar spacer attached between the heat spreader and the DBC completes the top electrical connection. Appropriate metals are deposited to achieve solderable connections on the heat spreader and kovar spacer. This approach, apart from eliminating the wire bond connections, also reduces the electrical resistances of

the package interconnections. This reduction allows higher current capability with reduced losses, and hence increases power density.

Figure 4 shows a comparison of the resistance for the emitter contact for different diameters of wire bonds and solder balls. The total resistance is the effective resistance seen for the 'n' number of wire bonds/solder balls for a given geometry. Clearly the resistance offered by the wire bonds is far higher than that of the solder balls. For the same diameter of 10 mils, the resistance of wire bonds is 120 times greater than that of solder balls. Figure 5 compares the total resistance of the wire-bonded module and the flip-chip package (MMC case). The device resistance is not shown as it is assumed the same for both cases and is excluded in the comparison. It shows that the total resistance of the wire-bonded module is 37 times greater than the one for the MMC case.

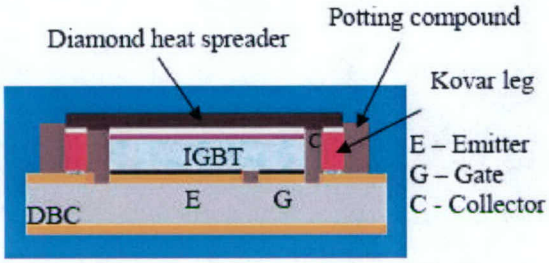

Figure 3. Diamond as a heat spreader for the proposed package.

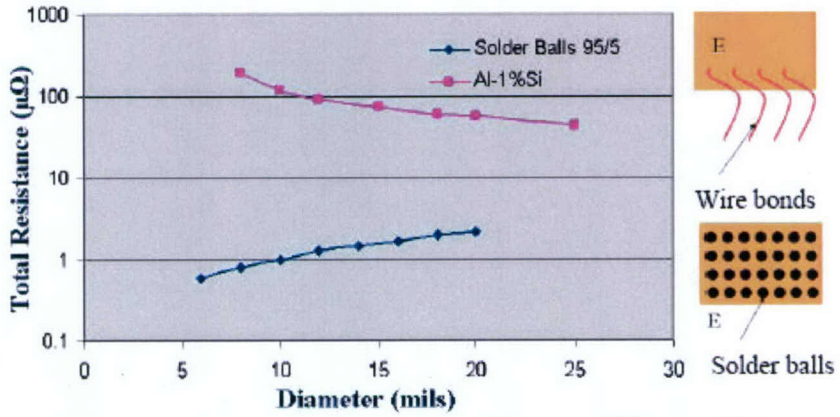

Die area = 15.6 mm x 15.6 mm

Figure 4. Comparison of resistance between wire bonds and solder balls.

III.2 Fabrication of the Test Vehicle

A test vehicle, consisting of a silicon-based thermal test die fabricated by the researchers and a CuMo heat spreader (35% Cu & 65% Mo), was used to evaluate the proposed packaging methodology. Table 1 shows the thickness, thermal conductivity K and Coefficient of Thermal Expansion (CTE) for different layers in the package that is closely CTE matched to maintain the mechanical integrity. The thermal test die mimics the steady-state losses in an IGBT and has embedded sensors to determine the temperature across the die. This is achieved through the use of integrated heaters and temperature sensors on the silicon die. The fabricated test die measured 15 mm x 15 mm and the CuMo heat spreader was 24 mm x 24 mm. A channel was milled in the heat spreader to accommodate the thermal test die and then the die was attached to the heat spreader using a high temperature solder. Later, the die was flipped and attached onto the DBC board using a low temperature solder. The completed test vehicle and its cross-sectional view are shown in Figures 6 and 7, respectively.

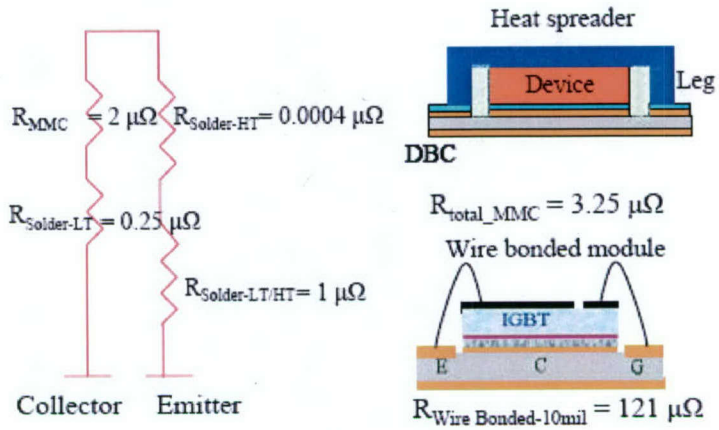

Figure 5. Comparison of the power package and wire bonded module.

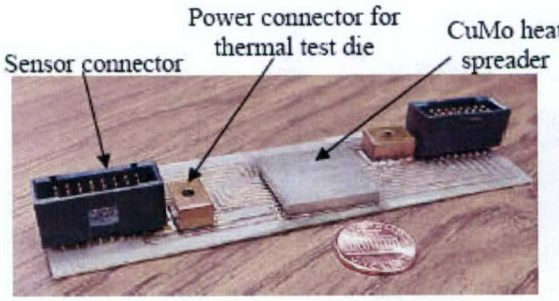

Figure 6. Completed test vehicle (CuMo).

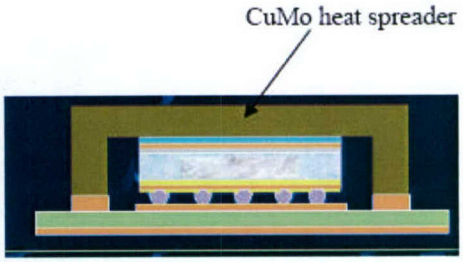

Figure 7. Sectional view of the CuMo package.

Table 1 Thermal and mechanical properties of various layers.

Interface	Material	Thickness (cm)	K (W/cm-K)	CTE (ppm/°C)
Die	Si	0.045	1.5	4
Solder	95Pb - 5Sn	0.005	0.23	30
	63Sn - 37Pb	0.005	0.5	25
Heat Spreader	65Mo – 35Cu	0.3	2.1	7.2
DBC	AlN	0.121	1.7	5

III.3 Fabrication of Flip-Chip Power Package using IGBTS for H-bridge Implementation

The fabrication of the power package can be divided into three major tasks:

- Processing of IGBT/diode wafers to achieve solderable metallization
- Processing of the substrate (DBC)
- Assembly of the package

III.3.1 - Processing of the IGBT/diode wafers

Whole wafers of the IGBT and diode die were obtained from International Rectifier. The IRG4PC30KD IGBT and diode die were selected because of their availability in wafer form and were compatible with the ratings of dc motors in the UAF Energy Conversion Laboratory. The nominal front metal composition (emitter side) for IGBT and diode (anode side) is 99% Al and 1% Si, which is suitable for wire bonding, and the backside metallization is Cr-Ni-Ag that can be soldered to a substrate using traditional solders such as Sn63. Figures 8 and 9 show the diode and IGBT wafers.

As aluminum is difficult to solder to, suitable metallizations are required for soldering the front metal during the flip chip process. Therefore, additional thin film processing of the obtained wafers was required. The major additional processing steps involved are listed below:

- Dicing of the wafer for processing only partial portions of the original wafer
- Zincating
- Electroless Nickel (EN) plating
- Dielectric coating (BCB/ Phtotoresist)
- Patterning of the dielectric layer according to the solder mask design

An EN plating process was chosen to plate globally the exposed metal pads as it *(a)* minimizes the number of process steps and *(b)* is less complicated. However, tight control of the plating bath is required for good adhesion of the nickel onto the plating surface. This means that a nickel plating bath along with a zincating bath were setup and tested on several test dies to check repeatability and process optimization. The bath consists of 25% by volume of the zincate concentrate (NaOH, zinc oxide and sodium gluconate) and 75% of distilled water. The zincating bath chemically removes the oxide layer on top of the aluminum and at the same time, a thin layer of zinc is coated on the aluminum to protect it from forming a native oxide layer. As the zincated sample is lowered into the EN plating bath, the zinc is etched away by the nickel solution and plating proceeds onto a pure clean Al surface. The EN bath consists of nickel sulfate (part A), sodium hypophosphite and ammonium hydroxide (part B) and water mixed in the ratio of 1:2:16. The bath temperature is maintained between 90-95 °C by a ceramic heater.

Once the process variables were optimized, the 6-inch IGBT wafer and 4-inch diode wafer were partially diced so the full wafer would not be damaged in case of a technical problem. Further time delays would have incurred if it had been necessary procuring a new whole wafer. The partial wafers were first zincated for about 25 seconds and were removed after the grayish appearance of zinc on the Al exposed pads. Full wafers can also be processed in this manner, however, this project only required a small number of dice in comparison to that available from a wafer, and the wafer cost is significant. Immediately the partial wafers were placed in the EN bath and plated for about 10 minutes to yield 5 to 6 microns of Ni. The EN plated wafers are then thoroughly rinsed and attached to a 5-inch Si carrier wafer using a double sided thermal release tape. This method allows to process wafers of non-conventional sizes. The wafers are spin coated with benzo-cyclo-butane, which is a dielectric liquid, and patterned according to the solder mask as shown in Figures 10 and 11. The solder mask opening size was evaluated from 6 to 9.5 mils, prior to selection of the 9-mils opening since this size resulted in the best reflow of the solder balls during assembly. The patterned partial IGBT/diode wafers are then diced to yield individual die. Figure 12 shows the diced IGBT and diode pieces.

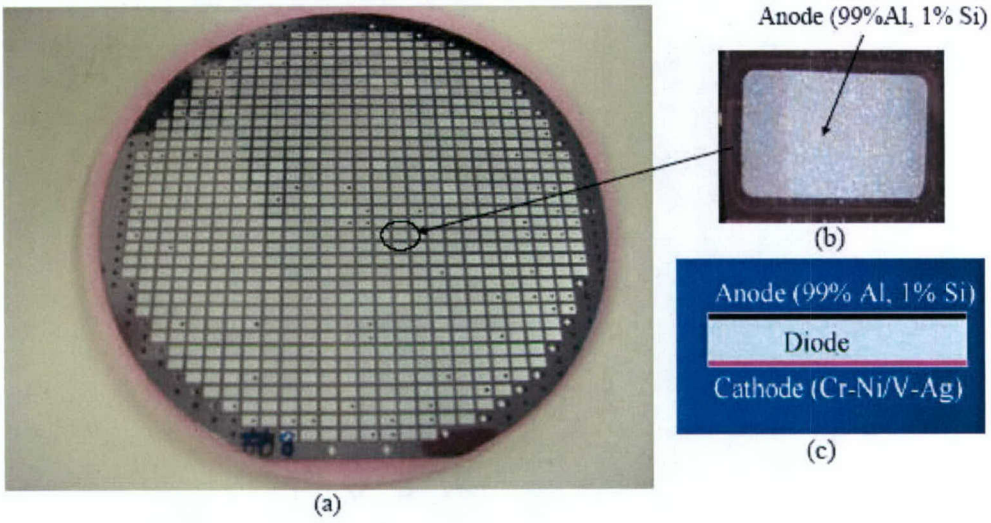

Figure 8. (a) Whole diode wafer (4-inch), (b) Bare die of a diode and (c) Sectional view of diode.

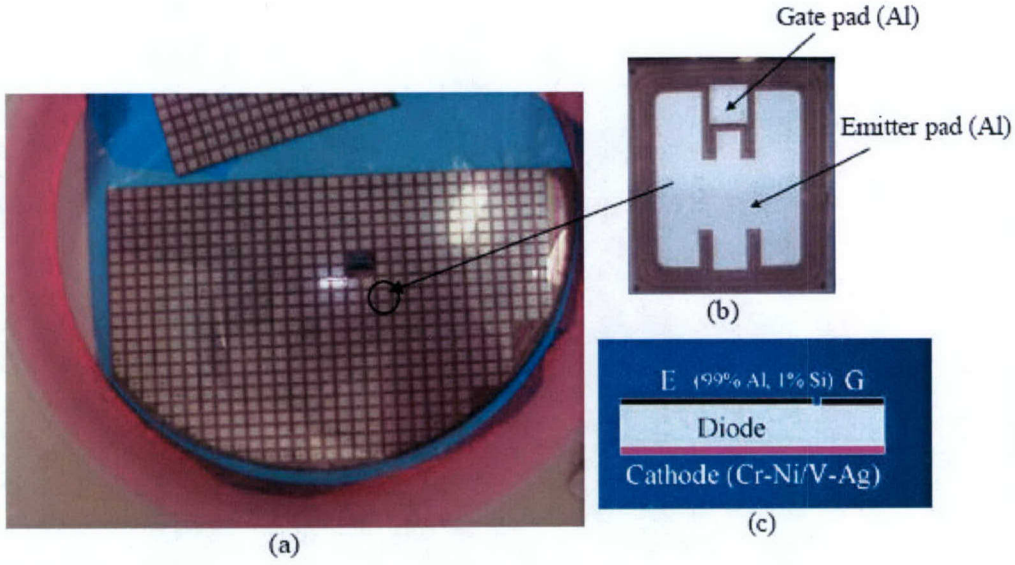

Figure 9. (a) Partially diced IGBT wafer (6 inch) for additional processing, (b) Bare die of an IGBT and (c) Sectional view of an IGBT.

III.3.2 - Processing of the substrate

DBC is one of the best choices for high current carrying requirements (up to 200 A). This is due to the low resistivity of copper and good thermal properties of DBC. The board consisted of dielectric (AlN or Al_2O_3) sandwiched between 12-mils of pure copper metallization on either side. The etching mask and the schematic for the H-bridge board are shown in Fig. 13.

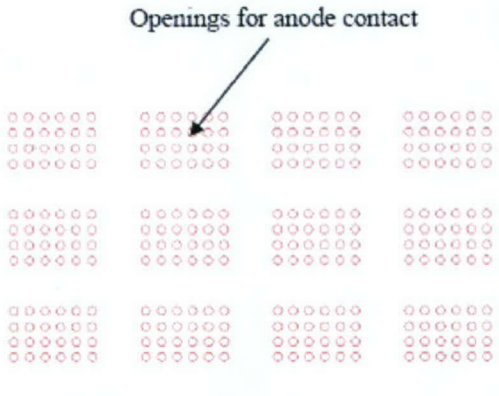

Figure 10. AutoCAD drawing of solder mask for diode.

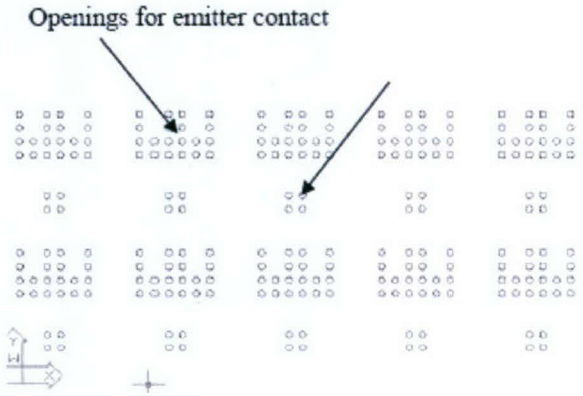

Figure 11. AutoCAD drawing of solder mask for IGBT.

A liquid photoimageable solder mask (TAIYO PSR-4000BN) was used to create a solder mask on the DBC boards. The solder mask opening size was optimized and an opening of 9 mils resulted in good adhesion of the solder balls onto the substrate. The pitch of the openings was selected as 16 mils, leaving a gap of 6 mils between two adjacent solder balls at the same electrical potential. Greater isolation values were achieved by simply spacing the solder balls an appropriate distance. The line spacing was governed by the spacing between the gate and emitter pad on the die and Figure 14 illustrates the line spacing issues. For 30-mils gate to emitter spacing on the substrate with an over etch of 4 mils, a row of solder ball openings were etched away when compared to the 15-mils design spacing with an over etch of 2 mils. A spacing of 15 mils was selected as it resulted in the maximum number of solder ball connections and therefore higher current handling capability.

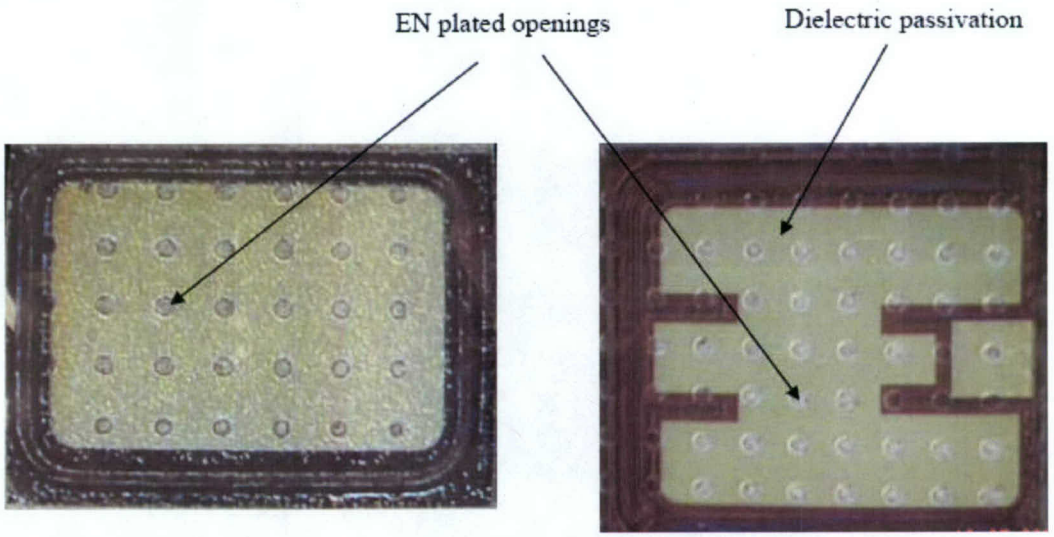

Figure 12. Diode/IGBT with passivation and solderable metallization.

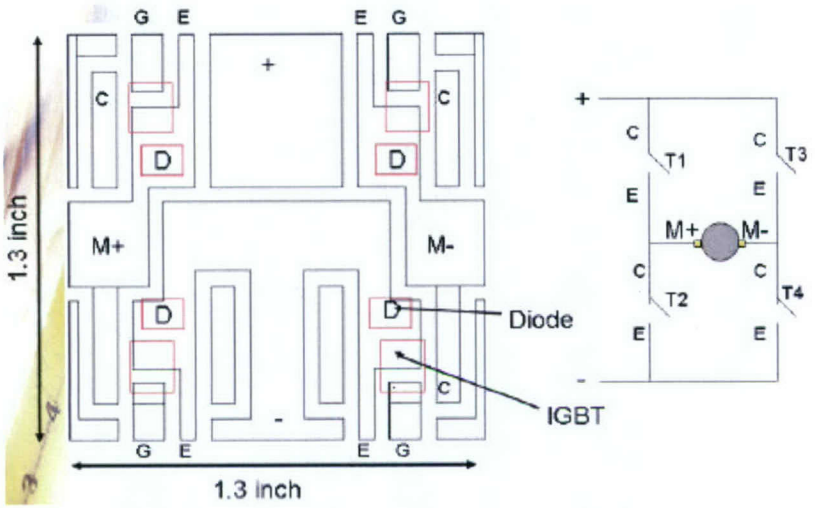

Figure 13. Schematic and physical layout of the H-bridge circuit.

III.3.3 Assembly of the power package

The temperature hierarchy of solder is the key for integrating the whole package (i.e. die, heat spreader and substrate). First, a set of four diodes and four IGBT dies were reflowed with high temperature 95Pb-5Sn solder balls (10 mils), see Figure 15. Then the four IGBT and diode pairs were flip chipped onto the DBC substrate, the kovar legs (19-mils thick) were also placed as shown in the Figure 16. The kovar legs were Ni plated (2 μm) and were reflowed along with the die using 95Pb-5Sn solder performs. The final stage of the assembly involves reflowing of heat spreader (AlN) onto the diode/IGBT pairs using a low temperature solder (Sn 63).

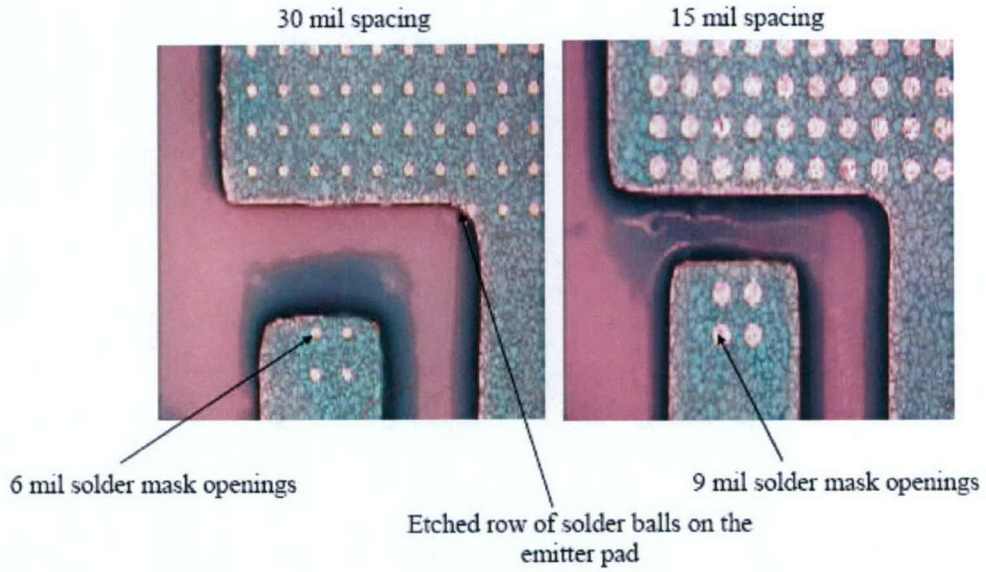

Figure 14. Minimum line spacing issues on the substrate.

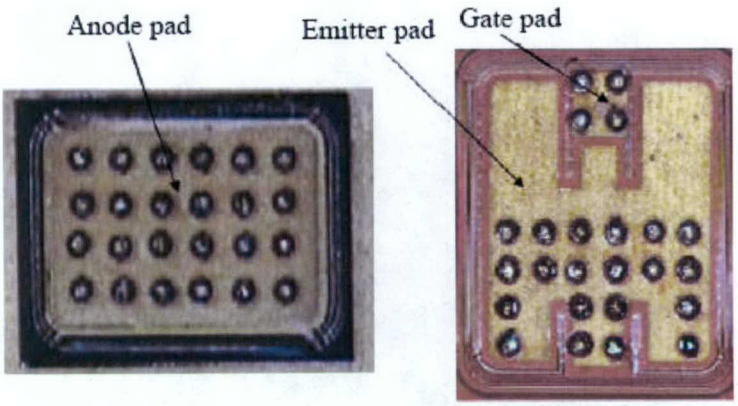

Figure 15. Solder balls reflowed on the Diode and IGBT respectively.

The side of AlN onto which the die will be attached was sputtered and finally plated with solderable metallization (Ti/Cu/ Ni). The size of the heat spreader was 11.58 mm x 9.7 mm. The power connectors (Cu blocks) were also soldered at this stage. Figure 17 shows the completed H-bridge power module.

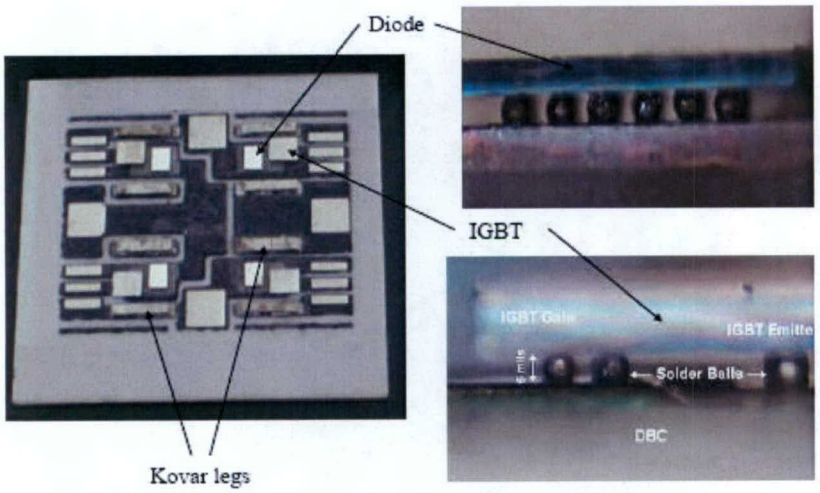

Figure 16. Assembly process of the die onto the substrate.

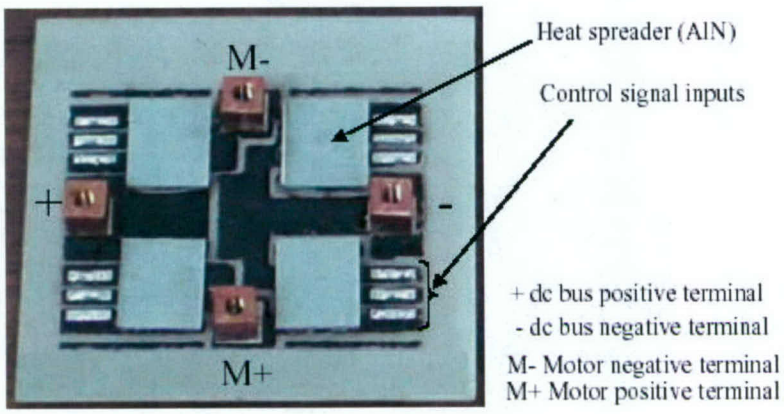

Figure 17. Completed 10 hp H-bridge power module.

IV. THERMAL ANALYSIS OF A SPRAY-COOLED POWER MODULE USING FLOTHERM

Thermal modeling of the developed spray-cooled H-bridge power module was performed to provide the researchers with useful information regarding the potential for any hot spots. This effort allowed the researchers to optimize the design before building prototypes. Unfortunately, there was no commercial CFD software package capable of simulating the two-phase change phenomenon taking place under spray cooling. Although commercial packages simulate single-phase cases, they can be used to estimate the temperature distributions and heat paths by assuming *(a)* a heat transfer coefficient at the heated surface impacted by the droplets (a value of 15,000 W/m^2-K was used), and *(b)* that the temperature in the chamber (where there is a mixture of droplets (fluid) and vapor (gas)) is constant (this temperature was selected as 40 °C to represent the worst case condition). The CFD package Flowtherm™ was used to perform the thermal simulations of the developed H-bridge power module simply because it was available to the researchers.

Using the device datasheet (i.e., part IRG4BC30KD from IR), the heat losses of the IGBT, P_{IGBT}, can be calculated from the total switching energy losses, E_{SW}, and conduction power losses, P_{CN}, as follows:

$$P_{IGBT} = E_{SW} f_{sw} + P_{CN} \tag{1}$$

$$P_{CN} = V_{CE(SAT)} I_C D \tag{2}$$

where f_{sw} is the switching frequency, $V_{CE(SAT)}$ is the IGBT collector-emitter saturation voltage, I_c is the IGBT collector current, and D is the duty cycle.

Similarly, the heat losses generated by the freewheeling diode, P_{DIODE}, are calculated from the diode reverse recovery losses, E_{rec}, and conduction losses, P_{CN_D}, as follows:

$$P_{DIODE} = E_{rec} f_{sw} + P_{CN\_D} \tag{3}$$

$$P_{CN\_D} = V_{ON} I_R (1 - D) \tag{4}$$

where V_{ON} and I_R are the on-state voltage and on-state current flowing through the freewheeling diode, respectively.

The material properties of the different blocks in the power module are the following:

Heat Spreader
- Material: AlN
- Dimensions: 11.58 mm x 9.68 mm x 0.625 mm
- Thermal Conductivity: 170 W/m-K
- Specific Heat: 725 J/kg-K

Standoffs
- Material: Kovar
- Dimensions: 2.0 mm x 9.68 mm x 0.7 mm
- Thermal Conductivity: 16.3 W/m-K
- Specific Heat: 439 J/kg-K

Solder
- Material: Sn63/Pb37
- Dimensions: 3.58 mm x 4.17 mm x 0.1 mm
- Thermal Conductivity: 51 W/m-K
- Specific Heat: 1500 J/kg-K

IGBT Bare Die
- Material: Silicon
- Dimensions: 3.58 mm x 4.17mm x 0.375 mm
- Thermal Conductivity: 151 W/m-K

- Specific Heat: 750 J/kg-K

Diode

- Material: Silicon
- Dimensions: 3.43mm x 2.54 mm x 0.3 mm
- Thermal Conductivity: 151 W/m-K
- Specific Heat: 750 J/kg-K

Solder Balls

- Material: Pb95/Sn5
- Radius (each one): 0.125 mm
- Number of Solder Balls: 8 x 36 = 288
- Thermal Conductivity: 51 W/m-K
- Specific Heat: 1500 J/kg-K

DBC Board

Material: Copper-AlN-Copper

Copper

- Dimensions:33 mm x 34.2 mm x 0.3 mm
- Thermal Conductivity: 385 W/m-K
- Specific Heat: 385 J/kg-K
- Electrical Resistivity: 3.2×10^{-8} Ohms-m

AlN

- Dimensions:33 mm x 34.2 mm x 0.625 mm
- Thermal Conductivity: 170 W/m-K
- Specific Heat: 725 J/kg-K
- Electrical Resistivity: 1.0×10^{12} Ohms-m

The gaps between the solder balls are filled with an underfill having a thermal conductivity of 1 W/m-K. Figure 18 illustrates a side view of the H-bridge power module implemented in Flowtherm to determine the different junction temperatures, T_j. By using the above formulae, heat losses (inputs on the Flowtherm simulations) were calculated for different switching frequencies and collector currents.

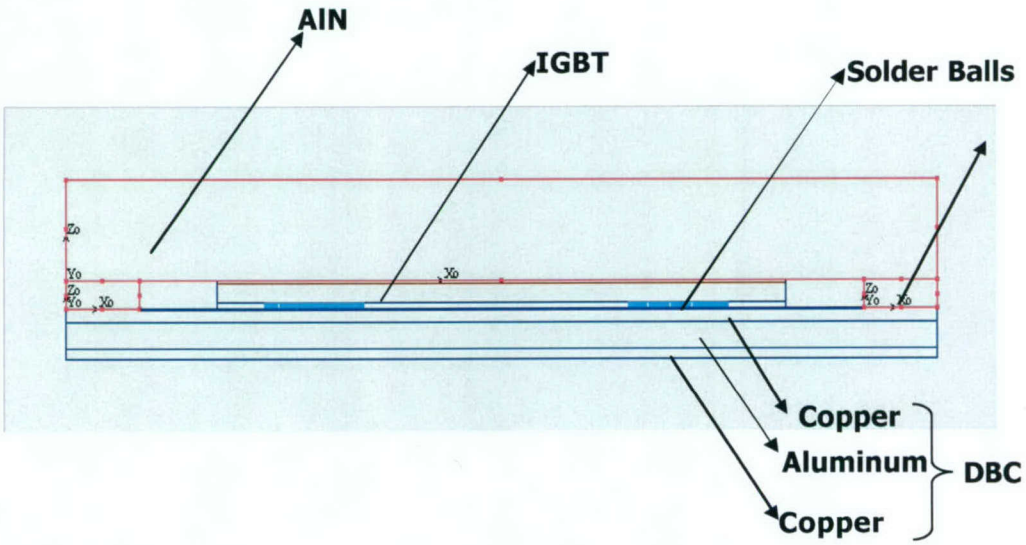

Figure 18. Side view of the thermal model

Figure 19 shows a typical Flowtherm output for the case of a collector current of 18 A and a switching frequency of 6 kHz. The motor is rotating in only one direction so two IGBTs were operating and their corresponding freewheeling diodes operated when these IGBTs were turned off. As expected the heat losses of the IGBTs were much greater than those of the freewheeling diodes.

Table 2 summarizes the results for switching frequencies of 6, 9, 12 and 15 kHz as well as collector currents of 10, 16, 18, 20 and 30 A. It is noted that 16 A is the maximum continuous collector current of the selected IRG4BC30KD IGBT for a case temperature of 100 °C. Table 2 highlights those operating conditions where a junction temperature of 125 °C was not exceeded. The maximum junction temperature specified by the manufacturer is 150 °C but the research team decided to adopt the limit of 125 °C due to safety reasons. For the IR-packaged IGBT, the maximum switching frequency is approximately 9.2 kHz for a collector current of 16 A, a junction temperature of 125 °C, an ambient temperature of 40°C and other data (e.g., thermal resistances) from its datasheet.

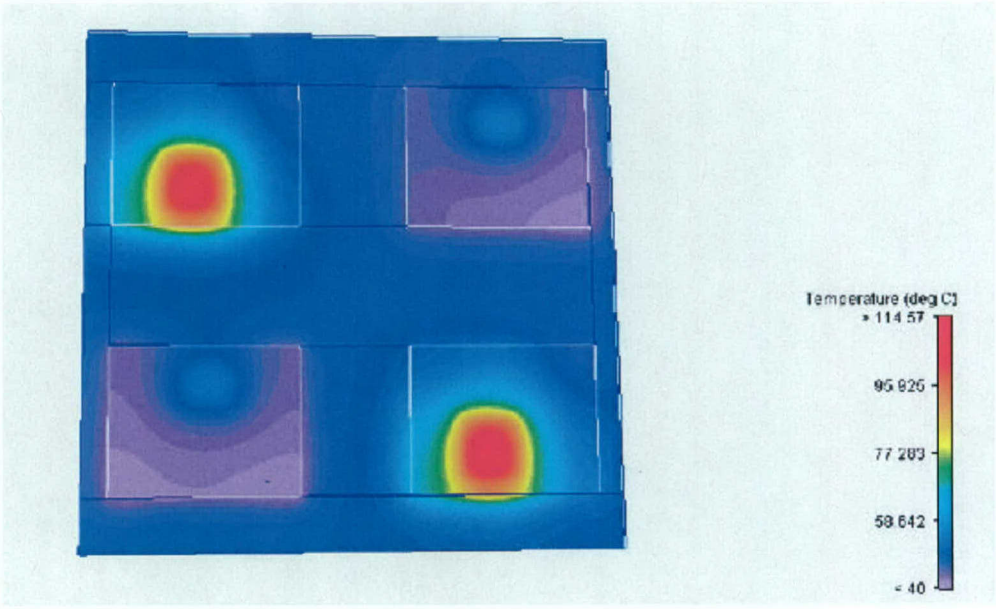

Figure 19. H-bridge temperature distribution for a collector current of 18 A at 6 kHz.

Table 2. Summary of the Flowtherm-based thermal simulations.

Total Losses and Junction Temperatures for a Single Spray-Cooled IGBT

I_c (A)	V_{ce}(sat) V	E_{sw} (mJ)	Total Losses at 6 kHz (W)	T_j at 6 kHz (°C)	Total Losses at 9 kHz (W)	T_j at 9 kHz (°C)	Total Losses at 12 kHz (W)	Tj at 12 kHz (°C)	Total Losses at 15 kHz (W)	Tj at 15 kHz (°C)
10	1.9	0.8	20	71.1	22.4	74.9	24.8	78.6	27.2	82.3
16	2.25	1.7	39	100.7	44.1	108.4	49.2	116.5	54.3	124.5
18	2.45	2	47.28	113.5	53.28	122.9	59.28	132.2	65.28	141.6
20	2.6	2.4	56	127.1	63.2	138.37	70.4	149.5	77.6	160.7
30	3.2	4.4	103.2	200.6	116.4	221.2	129.6	241.7	142.8	262.2

The continuous collector current specified by the manufacturer depends among other factors on the thermal resistances of the package, a TO-220AB package in this case. Spray cooling, by being more effective in extracting heat losses, may offer the possibility of increasing either the switching frequency or the current rating of the semiconductor device. From the table, spray cooling could enable operation at the higher switching frequency of 15 kHz for the rated current of 16 A and a junction temperature of 125 $^{\circ}$C; a significant increase in switching frequency. Alternatively, spray cooling could offer the possibility of operating the IGBT at a collector current of 18 A for a switching frequency of 9 kHz – the frequency limit for the TO-220AB package.

V. DESIGN OF A SPRAY COOLING BOX FOR A FOUR-SWITCH POWER MODULE

An innovative spray-cooling system illustrated in Fig. 20 was developed by the researchers in order to demonstrate the heat-removal capabilities of spray cooling. The system was designed to cool the H-bridge power module whose design and packaging methodology were addressed in Section III above. The H bridge is intended for driving a 240-V, 10-hp dc motor load.

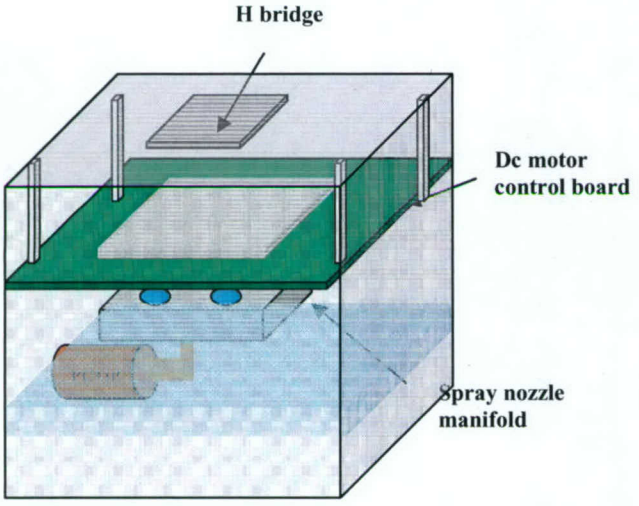

Figure 20. Graphical representation of the spray box.

In this innovative design, the spray box contains most of the system components allowing for a compact realization in order to maximize power and mass budgets. The spray box was made out of aluminum with an acrylic airtight lid. The fluid is contained at the bottom of the spray box and pumped to the nozzle manifold using a pump. A closed loop was formed by the fluid reserve at the bottom of the box, the pump, the nozzle manifold and the box walls acting as a condenser.

The outer dimensions of the spray box were 6.5" x 6" x 6" (HxWxD) with the H bridge and its control board mounted to the lid to allow accessibility. The motor control circuitry was fabricated on a FR-4 board and placed below the DBC board inside the spray box as illustrated in Figure 20. The motor control board has a 1.2" x 1.2" window (see Figure 21) to allow for the spray from the nozzle manifold to reach the H bridge located above and facing downwards. The manifold shown in Figure 22 was designed to allow one nozzle for each heat spreader (i.e., four nozzles in total) placed at the optimal distance below the H bridge (see Wei 2004).

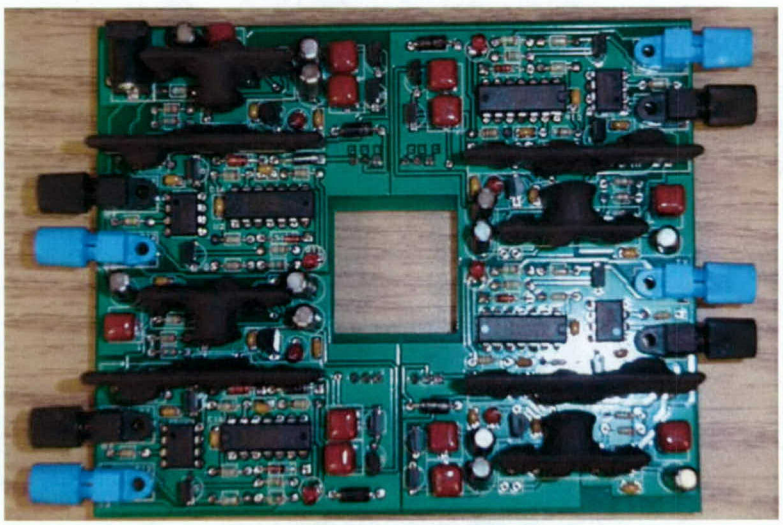

Figure 21. Gate driver board for the H bridge.

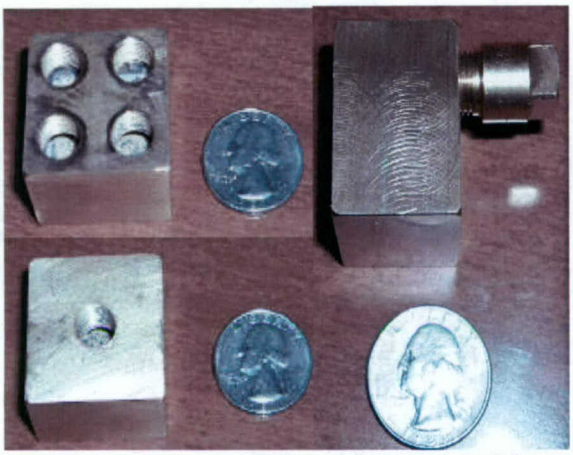

Figure 22. Spray nozzle manifold designed for cooling the H-bridge power module.

The nozzles were type 1/8HH-1 from Spraying Systems Co. (www.spray.com) having a nominal orifice diameter of 0.031", a length of 7/8", minimum pressure of 10 PSI, and maximum pressure of 150 PSI. A single nozzle is observed on the top right side of Figure 22. The airtight lid also contains the required power and fiber optic inputs for the electronics. IGBT gate signals were optically isolated from the dc motor controller. An observation window was located on one side of the spray box. The window, not necessary in a commercial product, added some height to the spray box. Figure 23 shows the spray box housing with it's observation window.

In a closed-loop system, the vapor that results when the sprayed fluid in the form of droplets impacts the heated surface (or device) and undergoes a phase change must be recovered by a condenser. Traditionally the two tasks of condensing the liquid and removing the heat are accomplished by adding a separate condensation coil and heat exchanger to the spray system. This methodology has proven to be effective but significantly increases the overall system size, thus reducing the overall system power density.

The proposed spray box achieves both tasks without the penalty of increased system size. This was accomplished by avoiding the use of a dedicated heat exchanger and condensation coil, using instead two ¼" cooling channels that were imbedded into the ½" walls of the spray box (not shown in Figure 20). The channels allowed chilled water to be connected to the spray box and circulated throughout the aluminum walls in a fashion very similar to that of a cold plate. The cooled walls were then used to subcool the fluid contained at the bottom of the spray box while condensing the liquid vapors present inside the box. The unique design of the spray box, in particular the walls, allows the system to maximize heat removal while also minimizing the size and weight of the spray-cooling system.

Figure 23. Completed spray box housing.

This system realization is different from other researchers where the spray-cooling system and the system containing the heat sources (the H bridge) are "packaged" separately yielding solutions requiring higher mass and volume budgets in addition to the additional thermal resistance of the separate package. The UAF approach consists of designing a spray box that becomes the "package" for the system containing the heat sources.

Before designing the H-bridge spray system, the researchers designed and developed a test bench to evaluate the feasibility of spray cooling for power modules. The Second Annual Report covered in detail this test bench (see also Wei 2004, Ortiz 1999 and Liu 2000). The main purposes of the test bench were to allow computation of key parameters such as heat flux (q") and device junction temperature, and to optimize the spray cooling system before designing the final system consisting of a spray-cooled power module with real power semiconductor devices.

The two main elements of the spray-cooling test bench are the test bed and the test vehicle. The test bed is based on a system originally used to spray VME cards. The system was modified to handle higher power, the use of conductive fluids and to allow quick changes in the experimental setup. A single spray nozzle is attached to a linear motor allowing simple adjustments of the spray distance. A variable speed motor drives the pump for the spray loop. This allows the flow rate through the spray nozzle to quickly be changed by altering the speed of the driving motor. A heater/chiller and heat exchanger were added to the spray loop enabling precise control of the fluid temperature. Previous work by the UAF researchers (see Wei 2004) indicated that the ability to control the temperature of the sprayed fluid is significant to achieve optimal heat removal. The test vehicle consists of thermal test die having the same area as the selected IGBT and mimicking its heat losses.

VI. EXPERIMENTAL RESULTS

The experimental results have been divided into two main groups. The first group summarizes the main spray cooling results that were obtained using *(a)* a thermal test die and the test bench, and *(b)* the spray box described in Section V. The goal of the test bench experimentation was to evaluate different type of nozzles, fluids, pressures and flow rates. The advantage of spray cooling is illustrated by comparing experimental results when an IGBT packaged by the manufacturer is cooled by *(i)* the spray-cooling system of Section V and *(ii)* a cold plate. The second group corresponds to experimental results related to spray cooling of IGBT bare die packaged as per the methodology given in Section III. The main goal here is to emphasize that the final thermal management solution must also take into account the packaging aspects if one is to fully realize the potentials of spray cooling.

VI.1 Experimental Results: Test Bench

Previous results that evaluated several spray nozzles from Spraying Systems enabled the researchers to select nozzle TG-1 since it yielded the best results for this application when using a mixture of Fluorinert™ FC72 and FC84 (see the Second Annual Report and Wei 2004). The saturation temperature of FC72 and FC84 are 56 °C and 80 °C, respectively. The saturation temperature of the mixture is not known but the boiling point of the mixture tends to be nearer to the fluid which is more volatile or has higher vapor pressure according to the manufacturer 3M; that is, FC72 (232 vs. 79 torr). The specific heat of both fluids is 1.05 (J/g-°C), the latent heat and density of FC-72 are 21 (cal/g) and 1.68 (g/cm^3), the latent heat and density of FC-84 are 19 (cal/g) and 1.73 (g/cm^3). The distance between the spray nozzle and the thermal test heater was varied along with spray pressure, flow rate and fluid temperature. The heat flux (q") was calculated from the observed data (see Mudawar 2001) as follows:

$$q'' = \frac{P_d}{A_{th}} \tag{5}$$

where P_d is the power dissipated by the thermal test heater and A_{th} is the cross area of the heater (i.e., 15 mm x 15 mm). In this case the sprayed area is equal to that of the test heater. Figure 24 illustrates a test heater fabricated by the UAF researchers. The power supplied to the test heater was slowly increased until it reached the maximum temperature of 150 °C. A heater/chiller and heat exchanger were used to control the temperature of the dielectric fluid being sprayed and thermocouples were used to measure the fluid temperature. Experiments verified that heat flux is maximized for given nozzle and test heater when the square thermal test heater was circumscribed by the circular spray pattern. Thus, the optimal distance is a function of the spray angle and heater dimensions (see Wei 2004); in particular:

$$d_{sp} = \frac{0.5\, w_{th}}{\tan(0.5\,\theta_{sp})} \tag{6}$$

where d_{sp} is the optimal spray distance, w_{th} the width of the square thermal test heater and θ_{sp} is the nozzle spray angle.

Figure 25 illustrates the effect of the fluid temperature upon the heat flux. Lower fluid temperatures (increased subcooling) resulted in higher heat fluxes. This may indicate that in addition to vaporization of the Fluorinert™, heat removal through conduction is an important component of the spray cooling observed in the test bench. The maximum heat flux q" was near 140 W/cm^2 at atmospheric pressure and a flow rate of 0.085 gpm for the TG-1 nozzle that has a 0.036" (36 mils) orifice.

Experiments were also conducted to determine the role of spray cooling in the overall heat removal of the system. The total heat flux of the system (q") can be expressed as the following:

$$q'' = q''_s + q''_c \tag{7}$$

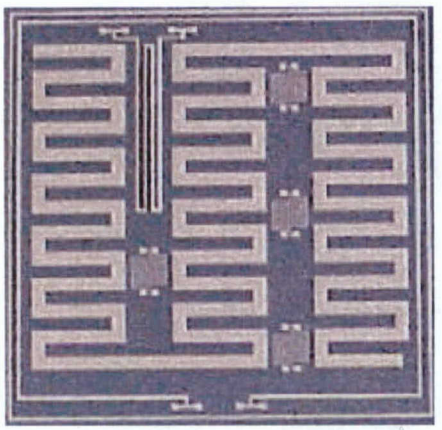

Figure 24. Individual test heater fabricated at UAF.

where q''_s is the heat flux associated with spray cooling while q''_c is the heat flux due to conduction losses through the backside of the silicon test heater, solder and substrate. Two packages were designed and built in order to determine the significance of the conduction losses. The first package utilized materials chosen to maximize the conduction losses. Highly conductive AlN DBC was chosen as the substrate and 95Pb-5Sn solder as the die attach material. The second package was designed to minimize the conduction losses. FR-4 was chosen as the substrate material and non-thermally conductive adhesive was used to attach the test heater. Both packages were spray cooled and their total heat fluxes are compared in Figure 26. The results indicated that just as high total heat fluxes were achieved with the package possessing minimal backside conduction as with the highly conductive package. These results support the assumption that the total system heat flux is predominantly a function of the heat removed as a result of spray cooling ($q'' \sim q''_s$).

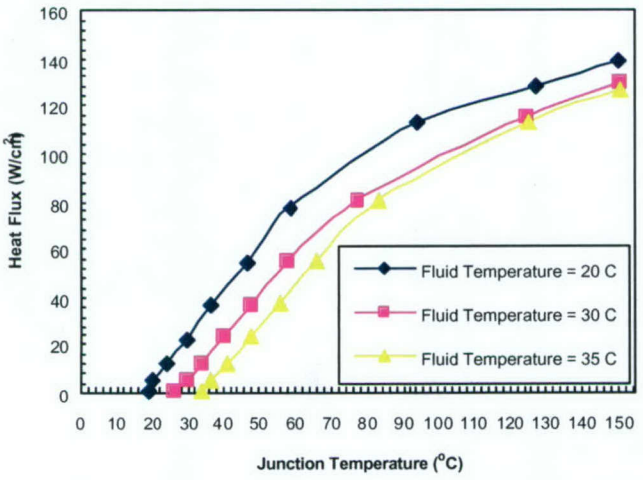

Figure 25. Effect of fluid temperature on heat fluxes as function of heater temperature.

Similar experiments were conducted leaving fluid temperature constant ($t_f = 20$ °C) and varying the flow rate. The results shown in Figure 27 indicate that increasing the flow rate led to higher heat fluxes while the other parameters remained constant. These experiments were performed using a single type of spray nozzle.

Similar experiments were performed where two similar nozzles having slightly different parameters were compared. The experiments compared a TG-1 nozzle (36 mil orifice diameter) and a TG-2 nozzle (47 mil orifice diameter). The results given in Figure 28 indicate that although the TG-2 has a larger capacity, thus allowing higher flow rates, nozzle TG-1 results in better heat fluxes. This indicates that the specific nozzle parameters such as orifice diameter, droplet size and droplet velocity play a significant role in determining the amount of heat flux achieved by the spray system. These results also indicate that conduction is an important component of the arrangement in the test bench. As mentioned in Section II above, there is no comprehensive theoretical model available at this time for the spray cooling phenomenon that can allow relating parameters like flow rate, nozzle orifice

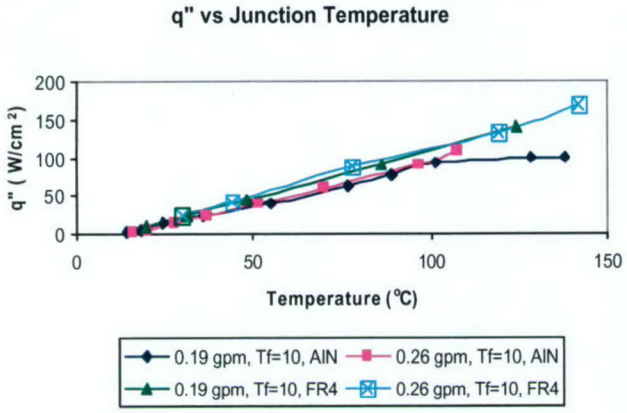

Figure. 26 Heat flux comparison of highly conductive (AlN) package and poorly conductive (FR-4) package.

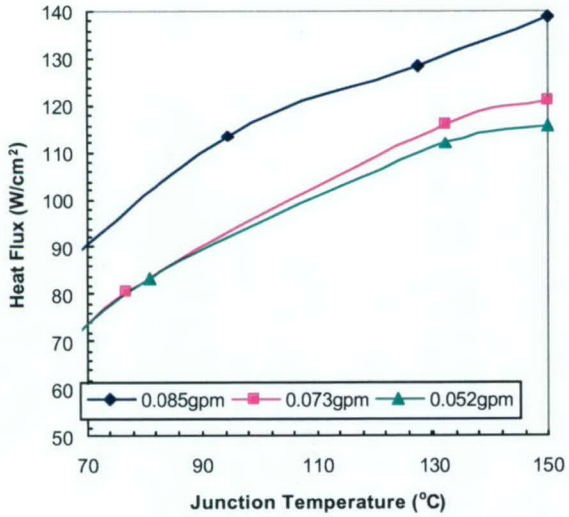

Figure 27. Effect of flow rate on heat fluxes as function of heater temperature.

and others into parameters like droplet size, droplet velocity and thin film thickness that are used for computer modeling. Making such a connection will be a goal of the next phase of this research project.

Power Packaging: Spray-Cooled Test Vehicle

The feasibility of the whole packaging methodology was first investigated using a low-cost test vehicle before applying the proposed packaging techniques using IGBT bare die (see Section III.2 above). The test vehicle consisted of a thermal test die and a heat spreader. The thermal test die mimicked the losses in the IGBT and had embedded sensors for determining the temperature across the die. Two packaging prototypes were used for the testing, one constructed with a diamond heat spreader and the other with CuMo heat spreader (35% Cu and 65% Mo). Each package was sprayed with a mixture of 50% FC-72 and 50% FC-84 dielectric fluids at standard atmospheric pressure, a flow rate of 0.19 gpm and a fluid temperature of 10 °C. The experimental results are displayed in Figure 29. Both packages resulted in maximum heat fluxes well over 100 W/cm^2 for a maximum temperature of 120 °C, with the diamond package exceeding 200 W/cm^2. These heat fluxes were calculated using die area as opposed to sprayed area (the latter is 2.56 larger). The setup successfully demonstrated the feasibility of the proposed spray cooling and packaging methodology. It was inferred from the test bench results that an atomized fluid that forms very fine droplets of the liquid produces superior results when compared to that of a high pressure "fire hose" type of spray. As a result the UAF researchers selected for the spray box (see Figure 23) the nozzle type 1/8 HH-1 that produced a finer spray than the nozzles used in the test bench experiments.

VI.2 Experimental Results: IR-Packaged IGBT

Bearing in mind that the main objective of this grant was to investigate the feasibility of using spray cooling as the thermal management technology for power semiconductor devices used in power converter applications, in particular, naval applications, the researchers setup a second test bench to drives a 240-V, 10-hp dc motor. Figure 30 is a photograph of the test bench. A dc power supply (rated 0-300 V and 50 A) is not shown in the figure.

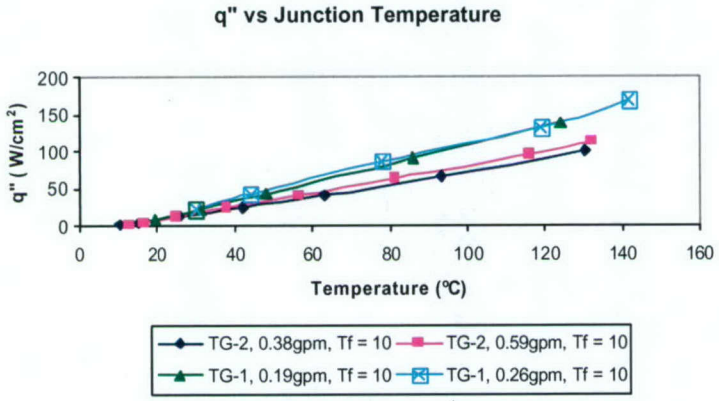

Figure 28. Effect of nozzle parameters on heat flux.

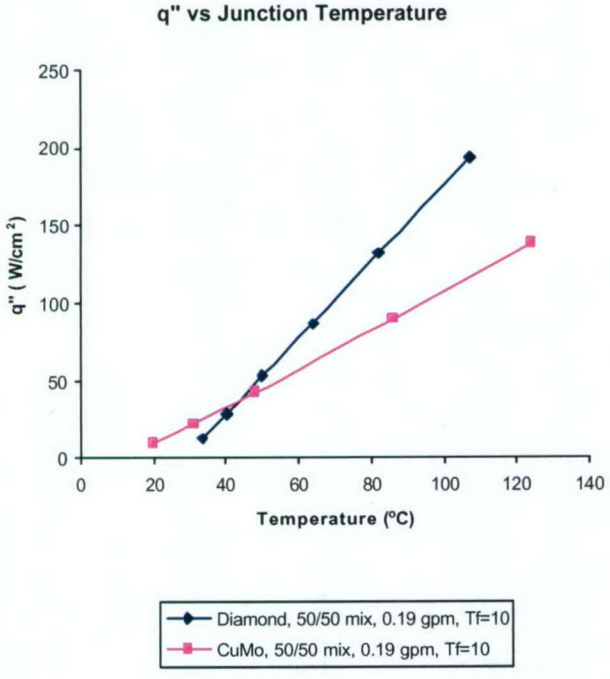

Figure 29. Heat fluxes when using diamond and CuMo heat spreaders (die area).

Laboratory experiments were conducted on a commercial TO-220AB package of the IGBT IRG4PC30KD using:

- The spray box (see Figure 23), and
- A standard cold plate (see Figure 31). The IGBT was attached to the cold plate via a thermal pad to provide electrical isolation and improve the thermal path (due to roughness of the cold plate surface).

For the sake of simplicity, only one switch was used to run the dc motor and the temperature of the chiller water was maintained at around 20 °C for both the spray-cooling and cold-plate experiments (the chiller is shown on the right side of Figure 30). A mixture of 50% FC-72 and 50% FC-84 dielectric fluids was used for the spray-cooling experiments.

Tables 3 and 4 depict the experimental results. The collector current, case temperature and spray temperature were measured. Power losses were calculated as mentioned in Section IV using switching losses and lowest on-state voltage from the IGBT datasheet. For the spray-cooling experiments the case temperature refers to that temperature measured on the other side of the surface where the liquid droplets impinge. That is, the side of the base plate where the bare die is attached (if one looks at the package with the base plate facing down one could see two areas having "half circle"

shape on the side of the package where the base plate is visible). The junction temperature was calculated using the measured case temperature and the case-junction thermal resistance from the IGBT datasheet. All calculated values were rounded off to their nearest integer values and the operating conditions common to both cases are highlighted in yellow. The cold plate measurements were stopped at 15 A because the measured case temperature was above 100 °C indicating that the junction temperature was higher than its maximum limit of 150 °C (as it was later calculated after completing the measurements). The spray-cooling measurements were stopped at 19.5 A because of a limitation of the dynamometer available in the Energy Conversion Laboratory.

Table 3. Spray-cooling data for IRG4BC30KD IGBT (IR packaged) at 9.2 kHz.

I_C(A)	T(case) (°C)	T(junction) (°C)	T(fluid spray) (°C)	P_{IGBT} (W)
0	21.0	21.0	19.2	0.0
5	23.6	39	19.3	13
10.4	26.8	59	19.9	27
15.2	31.7	79	20.5	40
16.5	33.2	85	20.9	43
19.5	36.3	97	21.5	51

Table 4. Cold-plate data for the IRG4BC30KD IGBT (IR packaged) at 9.2 kHz.

I_C(A)	T(case) (°C)	T(junction) (°C)	P_{IGBT} (W)
0	22.0	22	0
4.5	48.1	62	12
10	81.9	113	26
15	118.1	165	39

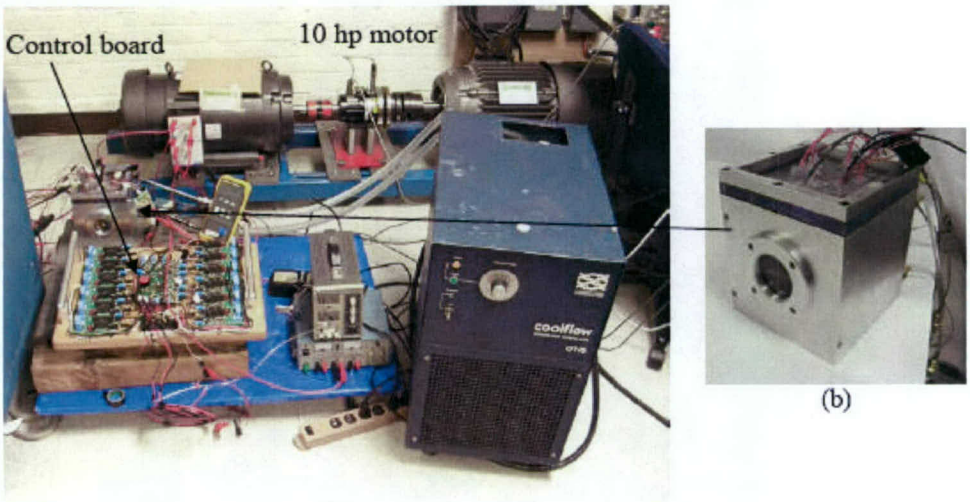

(a)

(b)

Figure 30. (a) Experimental setup for spray cooling of power devices, (b) Cooling chamber.

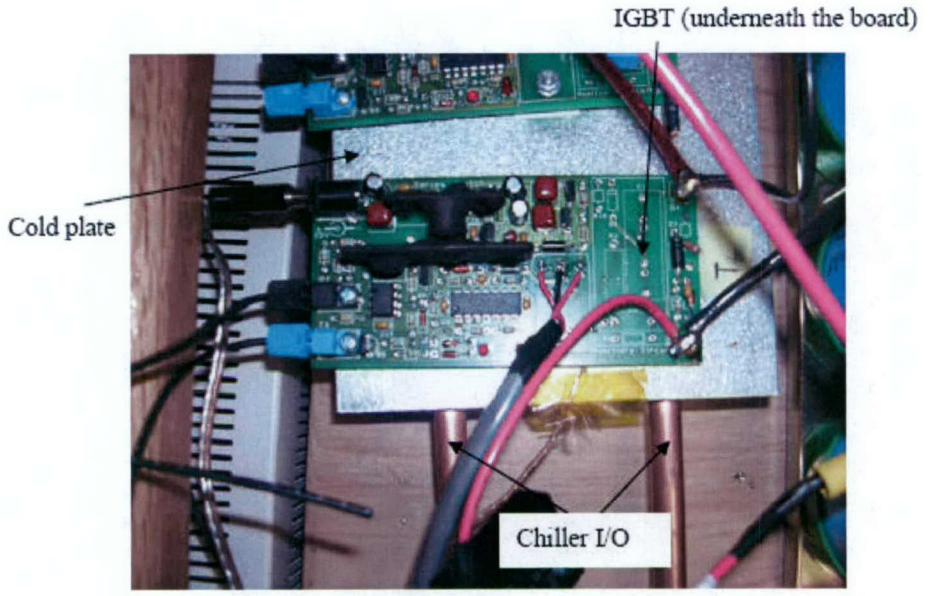

Figure 31. Experimental setup for liquid cooled cold plate.

Nevertheless, a comparison of the measured case temperature clearly shows the advantages of spray cooling; it was only 36.3 °C at a collector current of 19.5 A and a switching frequency of 9.2 kHz. The above operating condition would definitely be outside the manufacturer envelope when cooled by a heat sink or a cold plate. The measured case temperature for the cold-plate case is around 272% higher than the one for the spray-cooling case for approximately 15 A. This is a very important difference that could be used to either increase the switching frequency or the collector current of the IGBT. The reader is reminded that the maximum continuous collector currents specified by the manufacturer for the IRG4PC30KD are 16 A and 28 A at case temperatures of 100 °C and 25 °C, respectively.

VI.3 Experimental Results: UAF-Packaged Sprayed-Cooled IGBT

Table 5 illustrates the measured results when the IGBT bare die is packaged according to the proposed novel packaging methodology. As expected, the case temperature in Table 3 agrees well with the heat spreader temperature since the spraying conditions are identical. The main difference is in the calculated junction temperature that is considerably smaller for the UAF power package because it has been optimized for spray cooling. The junction temperature for the UAF power package is 33 °C, much lower than the 59 °C junction temperature of the TO-220AB package for identical power and spraying conditions. From these results one can envision that the UAF power package should be able to operate at higher power levels for the same junction temperature. Unfortunately, the UAF power package was render inoperable because of likely voltage spikes on the gate signals so it could only be tested to 10.2 A.

Table 5. Spray-cooling data for UAF power package at 9.2 kHz.

I_C(A)	T(heat spreader) (°C)	T(junction) (°C)	T(fluid spray) (°C)	P_{IGBT} (W)
0.0	20.3	21	20.0	0.0
5.1	22.5	25	20.1	13
10.2	26.7	33	20.8	27

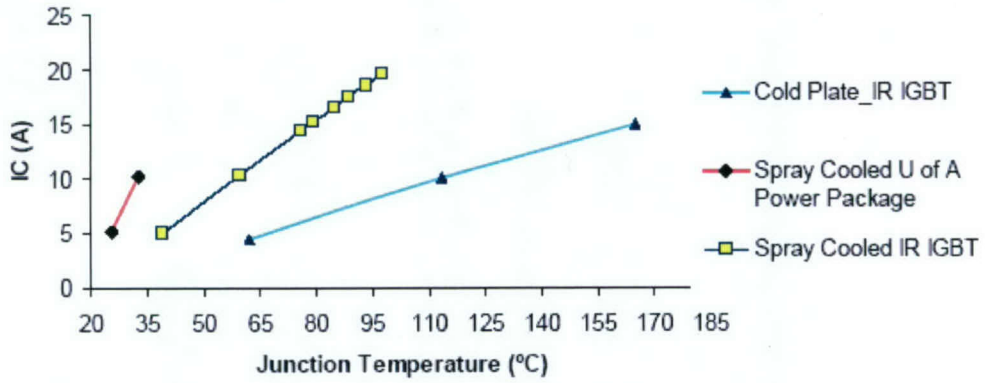

Figure 32. Collector current vs. junction temperature.

Working with actual IGBT (as opposed to using thermal test heater) brings considerable more risks and challenges. The experimental set up had significant amount of parasitic inductances that were causing over-voltages (see Figure 30). Measurements will be taken in future prototypes so this problem is not repeated. Nevertheless, this damage does not take away from the excellent performance of the UAF power package. At the writing of this report another UAF package is being developed for testing up to its maximum capability based on these promising results.

Figure 32 above illustrates in graphical form the results of Tables 3 to 5. An interesting point is that the junction temperature for the UAF power package is half of that for the IRG4PC30KD package for the same current levels. This was possible due to the lower thermal resistance value of the UAF power package built by the researchers (almost 4 times lower). Also, the UAF package area, for the same bare die, is almost 3 times smaller than that of the IR TO-220AB package. These results mean that potentially significant improvements in terms of power density and volume density could be possible by employing the novel packaging methodology developed by the UAF researchers. The thermal advantages of spray cooling over conventional cold-plate cooling are also extracted from Figure 32.

For completeness, Figure 33 illustrates typical measured gate signal, motor current, motor voltage and IGBT collector-emitter voltage. The electrical system was identical for both cases with the changes only taking place in the thermal management approach

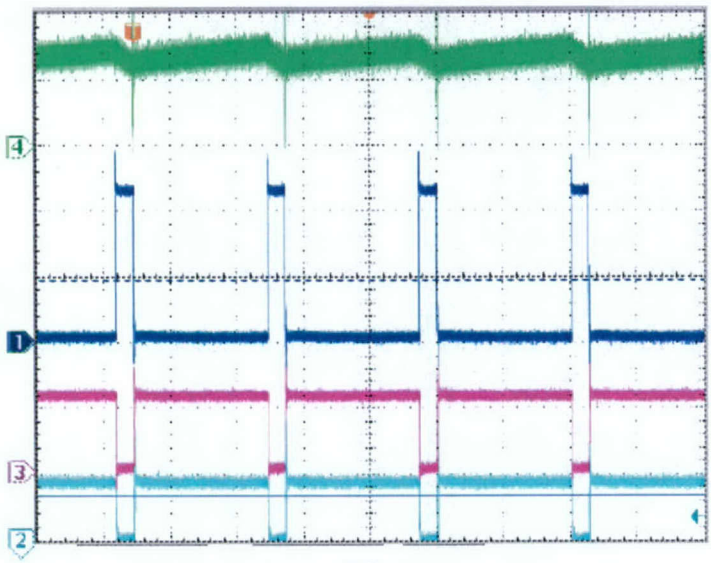

Ch1 V_{CE} (100 V/div)
Ch2 V_{GE} (20 V/div)
Ch3 V_{Motor} (200 V/div)
Ch4 I_C (10 A/div)

(a)

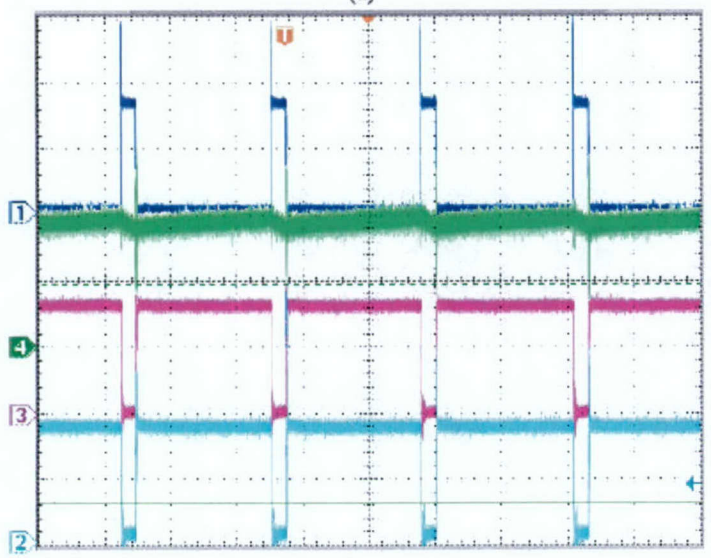

Ch1 V_{CE} (100 V/div)
Ch2 V_{GE} (10 V/div)
Ch3 V_{Motor} (100 V/div)
Ch4 I_C (10 A/div)

(b)

Figure 33. Typical measured signals for IR IGBT cooled by (a) Cold plate and (b) Spray cooling.

VII. CONCLUSIONS

The main objective was to investigate the feasibility of using spray cooling as the thermal management technology for power semiconductor devices used in power converter applications, in particular, naval applications. The main conclusions are addressed below in relation to enabling objectives established by the UAF researchers to accomplish the project main objective.

VII.1 Conclusions on Theoretical Understanding of Spray Cooling Phenomenon

Theoretical understanding of the basics of spray cooling modeling involving phase change was the first enabling objective since previous research efforts have been mainly experimental with little research done on a comprehensive modeling of the phenomenon. A comprehensive modeling of the spray cooling phenomenon could be used to design optimized spray cooling systems.

As a result of the literature survey the UAF researchers concluded that:

- The whole process of modeling phase change under spray cooling is a difficult task.
- Modeling of the heat transfer mechanism by a single droplet on a hot surface using a heat transfer coefficient and a CFD package has limited application because of the difficulty in determining the heat transfer coefficient under spray cooling from experimental work.
- Multiphase flow modeling is a viable technique to understand heat removal at the interfaces of liquid and solid by a vapor bubble.
- The "level set" method is one of the best methods to solve multiphase flow in spray-cooling systems. This conclusion resulted from a survey of the status of computer modeling in spray cooling and methods to solve multiphase flow model. The survey addressed in this report was published as a part of the Selvam (2005) paper.
- The modeling nucleation and the bubble growth in a thin film of liquid of about 70 μm should be performed in a future task.

VII.2 Conclusions on Power Packaging and Spray-Cooling of Power Semiconductor Devices

The enabling objectives on this topic focused on developing a power packaging methodology compatible with spray cooling since the UAF research team felt that packaging must be also considered when applying spray cooling in order to fully realize the benefits of this thermal management approach. A technology demonstrator consisting of an H-bridge power module driving a 240-V, 10-hp dc motor was assembled to demonstrate the feasibility of the proposed ideas.

Initially, the UAF researchers used thermal test heaters on a spray-cooling test bench to evaluate how factors such as pressure, flow rate and spray fluid temperature affect the cooling of the power semiconductor devices. The results demonstrated that in general:

- High nozzle flow rates are helpful when all other conditions are the same because of the enhanced conduction mechanism for heat removal.
- High-flow nozzles do not always produce the optimum cooling efficiency since they may hinder the phase-change process (see Figure 27).
- Droplet size, droplet velocity and perhaps other factors clearly play a key role in this process as it is being analyzed as part of ONR Award No. N00014-04-1-0603.

The UAF researchers designed a spray box to spray standard TO-220AB packages of the IRG4PC30KD part from International Rectifier (having an IGBT and a freewheeling diode) and the H-bridge power module packaged by the UAF packaging methodology (see Figure 23). The IRG4PC30KD

part was selected simply because of its availability in bare die form (so it could be packaged using the methodology of Section III) and its ratings were compatible with the electric motors available in the Energy Conversion Laboratory so experimental results could be conducted to practically demonstrate the feasibility of the proposed ideas. The IR-packaged part was also cooled under the same operating conditions by a standard cold plate for comparison purposes.

The experimental results demonstrated that:

- Spray cooling is much better than liquid cooling of a standard TO-220AB package.
- Simply spraying a conventional module does not result in the optimum cooling efficiency. The package must be also optimized. From an analysis of the experimental data, the performance of the spray-cooled UAF power package far exceeded the performance of the liquid- or even spray-cooled conventional package.

The UAF packaging methodology accomplished the following:

- Wired bonds, a major source of failure in power modules, were eliminated by replacing them with solder balls.
- The package materials were CTE matched for high reliability.
- The thermal resistance between the heat source and the liquid spray was significantly reduced with the potential of greatly improving the overall cooling efficiency.
- The technology can be used to implement chip-scale packages, thereby increasing the system power density.

In summary, the experimental results prove that spray cooling is an enabling thermal management technology that should meet the future heat load demands of power semiconductor devices used in power converters. However, novel packaging techniques such as the packaging methodologies developed by the UAF researchers are required to realize the full potential of spray cooling.

VIII. FUTURE WORK

Currently, several activities are underway as part of a continuation project that mainly concentrates on Silicon Carbide (SiC) power semiconductor devices (ONR Award No. N00014-04-1-0603). Regarding modeling the spray cooling phenomenon, these activities are aimed at developing a multiphase flow computer model using the level set method. The computer model will be used to study nucleation and boiling in a thin film of fluid of about 70-μm thickness on a hot surface. The UAF researchers are cooperating in the area of spray cooling with researchers from the Air Force Research Laboratory and NASA Goddard Space Flight Center.

While the results related to cooling of power semiconductor devices that were achieved in this ONR grant were a great improvement over many other methods of thermal management, the UAF researchers feel that potential exists to improve further the maximum heat flux that is possible with this technology. The current limitations are due to the properties of the used dielectric fluid and the fact that only a small portion of the sprayed fluid is converted to a vapor phase. Much of the fluid simply flows off the surface and contributes only to cooling by convection. On going work is focusing on the use of fluids with greater heats of vaporization values as well as methods to promote a more complete vaporization of the fluid. An important challenge is to be able to practically realize the theoretical concepts that promote greater vaporization of the fluid.

Current power packaging activities are aimed at packaging of SiC devices for high voltage and high temperature. The SiC MOSFET is being targeted for high voltage packaging and spray cooling will be used as the thermal management approach since it has a temperature limitation of approximately 200 °C

due to the gate oxide. The SiC JFET and SiC SIT are being targeted for high temperature packaging (greater than 250 °C or 300 °C).

REFERENCES

1. K. Azar (2002), "Advanced Cooling Concepts and Their Challenges", *Therminic 2002 (8th International Workshop on Thermal Investigations of IC and Systems)*, October 1-4, Madrid, Spain.
2. Q. Bai and Y. Fujita (1999), "Numerical simulation of the growth for a single bubble in nucleate boiling", Thermal Science & Engineering, 7, pp. 45-53.
3. E. Bigzadeh, F. Mignano (1995), "Experimental Determination of Heat Transfer Coefficient with Spray Cooling", *Proceedings of the ASME Heat Transfer and Fluids Engineering Divisions*, Vol. 233, pp. 73-88.
4. L.C. Chow, M.S. Sehembey and M.R. Paris (1997), "High heat flux spray cooling", *Annual Review Heat Transfer*, 8, pp. 291-318.
5. V. K. Dhir (2001), "Numerical simulation of pool-boiling heat transfer", *AIChE Journal*, 47, pp. 813-834.
6. M. DiMarzo et al. (1993), "Evaporative cooling due to a gravity deposited droplet", *International Journal of Heat Mass Transfer*, 36, pp. 4133-4139.
7. J.H. Ferziger and M. Peric (2002), Computational Methods for Fluid Dynamics, Springer, New York.
8. M.H. Gordon, G. Ni, W.F. Schmidt, and R.P.Selvam (1999), "A capillary-driven underfill encapsulation process", *Advanced Packaging*, pp. 34-37, April, 1999.
9. S. Haque, K. Xing, R-L. Lin, C. Suchicital, G-Q. Lu, D.J. Nelson, D. Borojevic, and F. C. Lee (1999), "An Innovative Technique for Packaging Power Electronic Building Blocks Using Metal Posts Interconnected Parallel Plate Structures," *IEEE Transactions on Advanced Packaging*, Vol. 22, No. 2, pp. 136-144.
10. Y. He, M. Shoji and S. Maruyama (2001), "Numerical study of high heat flux pool boiling heat transfer", *International Journal of Heat Mass Transfer*, 44, pp. 2357-2373.
11. D. Juric and G. Tryggvason (1998), "Computations of boiling flows", *International Journal of Multiphase Flow*, 24, pp. 387-410.
12. J. Kern and P. Stephan (2003), "Theoretical model for nucleate boiling heat and mass transfer of binary mixtures", *Journal of Heat Transfer*, 125, pp. 1106-1115 [Micro and macro region. Evaporation and bubble growth but no movement of the bubble].
13. J.P. Kizito, et al. (2004), "Numerical and experimental studies of splashing droplets", *42nd AIAA Aerospace Science Meeting and Exhibit,* AIAA-2004-0960 [splashing & thermal].
14. T. Kunugi (2001), "MARS for multiphase calculation", *CFD Journal*, 9, pp. 563-571.
15. R.C. Lee and J.E. Nydahl (1989), "Numerical calculation of bubble growth in nucleate boiling from inception through departure", *Journal of Heat Transfer,* 111, pp. 474-479.
16. L. Lin and R. Ponnappan, (2003), "Heat transfer characteristics of spray cooling in a close loop", *International Journal of Heat Mass Transfer*, 46, pp. 3737-3746.
17. S.P.Lin and R.D.Reitz (1998), "Drop and spray formation from a liquid jet", *Annual Review Fluid Mechanics*, 30, pp. 85-105.
18. X. Liu, S. Haque, and G-Q Lu (2001), "Three-Dimensional Flip Chip on Flex Packaging for Power Electronics Applications", *IEEE Transactions on Advanced Packaging*, Vol. 24, No. 1, February.
19. X. Liu, X. Jing, and G-Q. Lu (2000), "Chip Scale Packaging of Power Devices and its Application in Integrated Power Electronics Module", *Proceedings of the Electronic Components and Technology Conference*, ECTC'2000, Las Vegas, Nevada, May.
20. I. Mudawar (2001), "Assessment of high heat-flux thermal management schemes", *IEEE Transactions on Components and Packaging Technologies*, 24, pp. 122-141.
21. W. L. Ng, S. S. Ang, T. Thach, B. Ivy, F. Barlow, A. Elshabini, K. C. Burgers, K. J. Olejniczak, and W. D. Brown (2000), "Investigation of Wirebonds on Insulated-Metal Substrate for Multichip Power Module Applications", *International Conference on Microelectronics*, October, pp. 99-104.
22. L. Ortiz and J.E. Gonzalez (1999), "Experiments on steady-state high heat fluxes using spray cooling", *Experimental Heat Transfer*, Vol. 12, No. 3, pp. 215-233.

23. S. Osher and R. Fedkiw (2003), Level set methods and dynamic implicit surfaces, Springer, New York. Applies Mathematical Sciences: Vol. 153.
24. M. Pasandideh-Fard, S.D.Aziz, S. Chandra and J. Mostaghimi, (2001), "Cooling effectiveness of water drop impinging on hot surface", *International Journal of Heat Mass Transfer*, 22, pp. 201-210 [droplet dynamics- impact- shape of the film etc- thermal modeling & experiment].
25. C.O. Peterson (1970), "An experimental study of the dynamic behavior and heat transfer characteristic of water impinging upon a heated surface", *International Journal of Heat and Mass Transfer*, Vol. 13, pp.369-381.
26. M.M. Rahman, R. Mead, C.T. Hong, L. Lin and R. Ponnappan, (2004), "Numerical analysis of a spray nozzle for predictions of cone angle and pressure drop", *IECEC 2004: Proceedings of the 2nd International Energy Conversion Engineering Conference*, Rhode Island, Aug. 16-19.
27. D.P. Rini, R.H. Chen and L.C. Chow (2002), "Bubble behavior and nucleate boiling heat transfer in saturated FC-72 spray cooling", *Journal of Heat Transfer*, 124, pp. 63-72.
28. R. Scardovelli and S. Zaleski (1999), "Direct numerical simulation of free-surface and interfacial flow", *Annual Review Fluid Mechanics*, 31, pp. 567-603.
29. R.P. Selvam, and A.Elshabini (2000), "Nonlinear thermal stress and flow modeling in various electronic packages", *International Journal of Microcircuits & Electronic Packaging*, 23, pp. 224-233.
30. R.P. Selvam, L.Lin and R. Ponnappan (2005), "Computational modeling of spray cooling: Current status and future challenges", *Space Technology and Applications International Forum (STAIF 2005), Conference on Thermophysics in Microgravity*, Albuquerque, NM, Feb. 13-17, 2005.
31. M.C. Shaw, J.R. Waldrop, B. Chandrasekaran, B. Kagalwala, X. Jing (2002), "Enhanced Thermal Management by Direct Water Spray of High Voltage, High Power Devices in Three-Phase, 18-hp AC Motor Drive Demonstration", *2002 IEEE Intersociety Conference on Thermal Phenomena*, pp. 1007-1013.
32. S. Shin and D. Juric (2002), "Modeling three-dimensional multiphase flow using a level contour reconstruction method for front tracking without connectivity", *Journal Computational Physics*, 180, pp. 427-470.
33. G. Son, and V.K. Dhir (1998), "Numerical simulation of film boiling near critical pressures with a level set method", *Journal of Heat Transfer*, 120, pp. 183-192.
34. G. Son, V.K. Dhir and N. Ramanujapu (1999), "Dynamics and heat transfer associated with a single bubble during nucleate boiling on a horizontal surface", *Journal of Heat Transfer*, 121, pp. 623-631.
35. G. Son and N. Hur (2002), "A coupled level set and volume-of-fluid method for the buoyancy-driven motion of fluid particles", *Numerical Heat Transfer, B*, 42: pp. 523-542.
36. W. A. Srignano (1999), Fluid dynamics and transport of droplets and sprays, Cambridge University Press, England.
37. P. Stephan and J. Hammer (1994), "A new model for nucleate boiling heat transfer", *Heat Mass Transfer*, 30, pp. 119-125.
38. M. Sussman, P. Smereka and S. Osher, (1994), "A level set approach for computing solutions to incompressible two-phase flow", *Journal Computational Physics*, 114, pp. 146-159.
39. G. Trggvason et al. (2001), "A front-tracking method for the computations of multiphase flow", *Journal Computational Physics*, 169, pp. 708-759.
40. K. Vanam, J. Junghans, F. D. Barlow, R. P. Selvam, J. C. Balda, A. Elshabini (2005), "A Power Packaging Methodology for Spray Cooling of Power Semiconductor Devices using Dielectric Liquids", *20th Annual IEEE Applied Power Electronics Conference (APEC'05).*, March 6-10, Austin (TX), pp. 2014-2018.
41. Y. Wei, J. Junghans, J. C. Balda, F. D. Barlow, A. Elshabini (2004), "Some Considerations for High Power Motor Drive Systems for Ship Propulsion", *Electric Machine Technology Symposium 2004 (EMTS 04)*, Philadelphia (PA), January 27-29.
42. S.W.J. Welch (1998), "Direct simulation of vapor bubble growth", *International Journal of Heat Mass Transfer*, 41, pp. 1655-1666.

43. S.W.J. Welch and J. Wilson (2000), "A volume of fluid based method for fluid flows with phase change", *Journal Computational Physics*, 160, 662-682.
44. J. Yang, L.C. Chow and M.R. Paris (1996), "Nucleate boiling heat transfer in spray cooling", *Journal of Heat Transfer*, 118, pp. 668-671.
45. H.Y. Yoon, S. Koshizuka and Y. Oka (2001), "Direct calculation of bubble growth, departure, and rise in nucleate pool boiling", *International Journal of Multiphase Flow*, 27, pp. 277-298.